Geophysical Journal International

Geophys. J. Int. (2010) **182,** 113–136 doi: 10.1111/j.1365-246X.2010.04635.x

Characterization of sills associated with the U reflection on the Newfoundland margin: evidence for widespread early post-rift magmatism on a magma-poor rifted margin

Gwenn Peron-Pinvidic,[1]* Donna J. Shillington[2] and Brian E. Tucholke[3]

[1]*IPGS-EOST-UdS,* 1 *rue Blessig,* 67084 *Strasbourg Cedex, France. E-mail: gwenn.peron-pinvidic@ngu.no*
[2]*Lamont-Doherty Earth Observatory, Columbia University, P.O. Box* 1000, 61 *Route* 9W, *Palisades, NY* 10964, *USA*
[3]*Woods Hole Oceanographic Institution, Woods Hole, MA* 02543-1541, *USA*

Accepted 2010 April 17. Received 2010 April 15; in original form 2009 April 21

SUMMARY

Drilling during ODP Leg 210 penetrated two post-rift sills (dated as ∼105.3 and ∼97.8 Ma) in the deep sediments overlying basement of the continent–ocean transition zone on the magma-poor Newfoundland margin. The sill emplacement post-dated the onset of seafloor spreading by at least 7–15 Myr. The shallower of the two sills coincides with the high-amplitude U reflection observed throughout the deep Newfoundland Basin, and strong reflectivity in the sub-U sequence suggests that a number of other sills are present there. In this paper, we use multichannel seismic reflection data and synthetic seismograms to investigate the nature, magnitude and extent of this post-rift magmatism in the deep basin. Features observed in seismic profiles that we attribute to sill injection include high-amplitude reflections with geometries characteristic of intrusions such as step-like aspect; abrupt endings, disruptions and junctions of reflections; finger-like forms; differential compaction around possible loci of magma injection and disruption of overlying sediments by apparent fluid venting. Interpreted sills occur only over transitional basement that probably consists of a mixture of serpentinized peridotite and highly thinned continental crust, and they cover an area of ∼80 000 km^2. From analysis of synthetic seismograms, we estimate that sill intrusions may comprise ∼26 per cent of the sub-U high-reflectivity sequence, which yields a crude estimate of ∼5800 km^3 for the total volume of sills emplaced by post-rift magmatism. This is significant for a margin usually described as 'non-volcanic'. We discuss competing hypotheses about the source of the magmatism, which is still uncertain.

Keywords: Ocean drilling; Continental margins: divergent; Hotspots; Atlantic Ocean.

1 INTRODUCTION

The Newfoundland–Iberia conjugate margins (Fig. 1a) are among the best-studied magma-poor rifted margins in the world. They have been the focus of four legs of the Ocean Drilling Program (ODP) (Legs 103, 149, 173 and 210) (Boillot *et al.* 1987a; Sawyer *et al.* 1994; Whitmarsh *et al.* 1998; Tucholke *et al.* 2004) and numerous geophysical experiments for more than two decades. The studies have consistently shown that continental breakup was accompanied by very little syn-rift magmatism. Instead, mantle that is at least partly subcontinental was exhumed in the continent–ocean transition, as demonstrated by recovery of serpentinized peridotite from basement highs that have been drilled on both margins (Boillot *et al.* 1987b; Cornen *et al.* 1996; Abe 2001; Hébert *et al.* 2001; Müntener & Manatschal 2006). Wide-angle seismic reflection and refraction studies indicate that these mantle exposures may extend 200 km or more orthogonal to the margins (Dean *et al.* 2000; Funck *et al.* 2003; Lau *et al.* 2006b; Van Avendonk *et al.* 2006). The mantle exposures have been referred to as the Zone of Exhumed Continental Mantle (ZECM) (Whitmarsh *et al.* 2001) or as 'transitional basement' because they are neither continental crust nor typical oceanic crust. The combined exhumation of mantle and paucity of significant syn-rift magmatism have usually been attributed to relatively slow and cold rifting (e.g. Bown & White 1995).

Although the rifting itself was magma-limited, significant volumes of magmatic rocks that postdate rifting by up to ∼15 Myr are found around the Newfoundland margin (Pe-Piper *et al.* 1994). Drilling during ODP Leg 210 in the Newfoundland Basin also encountered evidence for early post-rift magmatic activity. Two post-rift sills dated at ∼105.3 and ∼97.8 Ma (middle Albian

*Now at: NGU, Geological Survey of Norway, Leiv Eirikssons vei 39, 7491 Trondheim, Norway.

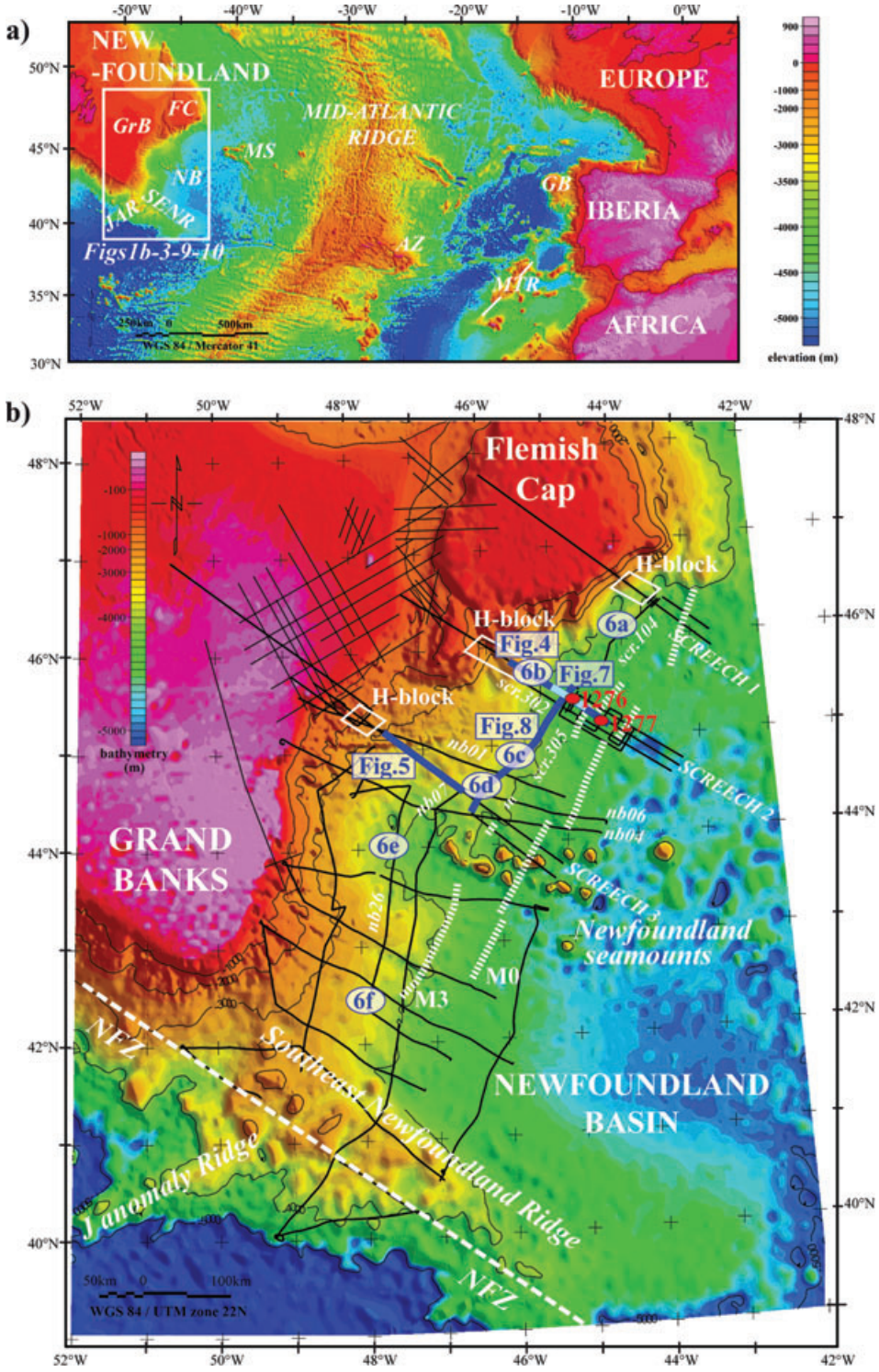

Figure 1. (a) Bathymetric map showing the conjugate Newfoundland and Iberia margins in the North Atlantic Ocean. AZ, Azores; FC, Flemish Cap; GB, Galicia Bank; GrB, Grand Banks; JAR, J Anomaly Ridge; MS, Milne Seamounts; MTR, Madeira-Tore Rise; NB, Newfoundland Basin; SENR, Southeast Newfoundland Ridge. (b) Bathymetry of the Newfoundland margin with contours at 1000 m intervals. Lines show MCS reflection profiles studied, and thick blue lines and white circles locate profiles illustrated in Figs 4–8. Red dots locate ODP Sites 1276 and 1277. Dashed white lines show magnetic anomalies M0 and M3 (Srivastava *et al.* 2000). scr, SCREECH profiles; nb, R/V Conrad profiles. All bathymetric data are from the NGDC, Smith and Sandwell compilation.

and early Cenomanian) were encountered in deep sediments (~1610–1720 mbsf) that closely overlie transitional basement at Site 1276 (Fig. 1b) (Tucholke *et al.* 2004; Hart & Blusztajn 2006). Shillington *et al.* (2007) demonstrated that the sills correlate with high-amplitude reflections in multichannel seismic reflection (MCS) data, with the shallower of the two sills emplaced at the level of a regional seismic marker termed the U reflection. The U reflection is very strong throughout the deep Newfoundland Basin,

and it often overlies deeper high-amplitude reflections (Tucholke *et al.* 1989); these features suggest that there was large-scale sill injection both at and below U in the post-rift sediments.

In this paper, we investigate the post-rift sill magmatism in the Newfoundland Basin using MCS data obtained during the SCREECH experiment in 2000 (Hopper *et al.* 2004; Lau *et al.* 2006a; Shillington *et al.* 2006), older academic MCS data (Tucholke *et al.* 1989), and open-filed industry MCS profiles obtained from the Canada Newfoundland Offshore Petroleum Board (Fig. 1b). We interpret the distribution and configuration of sills based on seismic reflection characteristics in the MCS records, and we use synthetic seismograms to estimate the thickness of the intrusions. These analyses are used to constrain the volume, extent, and timing of post-rift magmatism. Finally, we examine hypotheses for the possible source of the magmatism.

Determining the above parameters is important for understanding the geology and resource potential of the deep Newfoundland margin. Sills at the level of the U reflection should produce a marked impedance contrast with overlying sediments, potentially attenuating signal penetration to deeper levels. Analysis of smoothed instantaneous frequency and amplitude at the U reflection around ODP Site 1276 suggests that sills strongly inhibit signal penetration (Shillington *et al.* 2008). Thus, widespread distribution of sills might explain why the underlying surface of transitional basement generally is poorly resolved in MCS data (Tucholke *et al.* 1989) and why the basement often appears to be seismically transparent (Lau *et al.* 2006a; Shillington *et al.* 2006). In addition, it should be noted that the sills at ODP Site 1276 were intruded into 'black shales' intermittently enriched in organic carbon, and sills near the level of the U reflection would have intruded similar sediments elsewhere within the Newfoundland Basin. The scale and timing of thermal effects associated with these intrusions thus have significant implications for maturation of potential hydrocarbon resources.

2 GEOLOGICAL BACKGROUND

2.1 Rifting history

The Iberia–Newfoundland magma-poor margins record a complex tectonic history in which rifting was influenced in part by structure inherited from closure of the Iapetus and Rheic oceans during the middle to late Paleozoic (for a review, see Tucholke & Sibuet 2007; Tucholke *et al.* 2007). Two major rift phases can be distinguished (Late Triassic and Late Jurassic to Early Cretaceous) during which extensional deformation was accommodated along different parts of the margins. During the earlier phase, extension occurred in a wide-rift mode, and large, deep-rift basins formed in domains that are now in proximal (inboard) margin positions (e.g. Jeanne d'Arc, Carson, Horseshoe, and Lusitanian basins) (e.g. Enachescu 1988; Tankard *et al.* 1989; Driscoll *et al.* 1995). During the later phase, extension migrated toward and finally focused at distal (present-day seaward) parts of the margins, thinning the crust and exhuming subcontinental mantle in the continent–ocean transition zone.

The extent of exhumed mantle within the rift and the degree of magmatism associated with its emplacement are still debated. Based on modelling of magnetic anomalies, Whitmarsh & Miles (1995); Russell & Whitmarsh (2003) suggested that oceanic crust started to form in Barremian time (anomaly M5–M3, ∼130 Ma). Wilson *et al.* (2001) proposed an older, early Valanginian age (∼138 Ma) for the 'end of rifting', based on their interpretation of structural and stratigraphic architecture of the southern margin of Galicia Bank (note that throughout this paper we use the timescale of Gradstein *et al.* 2004; thus, ages quoted here may differ from those in cited papers). Tucholke *et al.* (2007) used drilling and seismic reflection/refraction data to show that rifting of continental crust between Flemish Cap and Galicia Bank continued to near the end of Hauterivian time (∼130 Ma), with mantle probably being exhumed farther to the south within the rift; they proposed that this was followed by exhumation of subcontinental mantle in at least parts of the rift until the end of Aptian time (∼112 Ma) when relatively normal seafloor spreading is interpreted to have started. Finally, Peron-Pinvidic *et al.* (2007) proposed that in these deep settings, oceanic accretion gradually developed in the zone of exhumed continental mantle from ∼128Ma and that 'final break-up' could be associated to a basin-wide tectono-magmatic event dated near the Aptian-Albian boundary (∼112Ma).

Within the sedimentary column on both the Newfoundland and Iberia margins, a pronounced reflection event correlates with the end of Aptian time (the 'Aptian event' of Tucholke *et al.* 2007). On the Newfoundland margin, this is the U reflection. The reflection can be traced onto the Grand Banks, where it merges with the mid-Cretaceous Avalon Unconformity (Grant 1977; Tucholke *et al.* 1989). In the deep Newfoundland basin the U reflection is intimately associated with igneous sills, as will be discussed below. Off Iberia, a well-defined and stratigraphically equivalent reflection (the 'orange reflection' of Groupe Galice 1979) is observed. This reflection, however, is generally much weaker than the U reflection, and it shows no association with igneous rocks where it has been penetrated by ODP drilling (Groupe Galice 1979; Rehault & Mauffret 1979). The fact that the U reflection in the Newfoundland Basin is overprinted by sill injection while there was no equivalent igneous activity off Iberia indicates that there was marked asymmetry in post-rift magmatism on the conjugate margins.

2.2 Record of magmatism

Most known magmatism associated with rifting between Newfoundland and Iberia was widely scattered and volumetrically minor (Fig. 2); the magmas were emplaced as dikes, sills, veins, and minor extrusives. Very little magmatism was associated with the Triassic rift phase. Magmatic activity was more common during the Late Jurassic–Early Cretaceous phase, although it was still scattered and very limited, and it concentrated on the Newfoundland side of the rift. A significant exception was the formation of the J-Anomaly Ridge and Southeast Newfoundland Ridge on the North American plate, together with the conjugate Madeira-Tore Rise on the EurAfrican plates (Fig. 1a). These edifices (collectively the JAR-MTR) are interpreted to have formed above a plume at the southern margin of the rift (red ellipse, Fig. 2) (Tucholke & Ludwig 1982), and they were emplaced in Barremian to early Aptian time (anomaly ∼M4 to younger than M0). The associated thick volcanics are thought to explain the high-amplitude 'J' magnetic anomaly (M1–M0) centred at the southern margin of the rift (Rabinowitz *et al.* 1978). The amplitude of this anomaly slowly decreases over distances of hundreds of kilometres to both the north and south, consistent with decreasing volcanism with distance from the plume. The anomaly reaches normal amplitude near the latitude of the southern margin of Galicia Bank and the conjugate Flemish Cap, suggesting that this was the northern limit of the magmatic influence (Tucholke *et al.* 2007).

The limited magmatism associated with Late Jurassic to Early Cretaceous rifting may have been sharply reduced at the end of

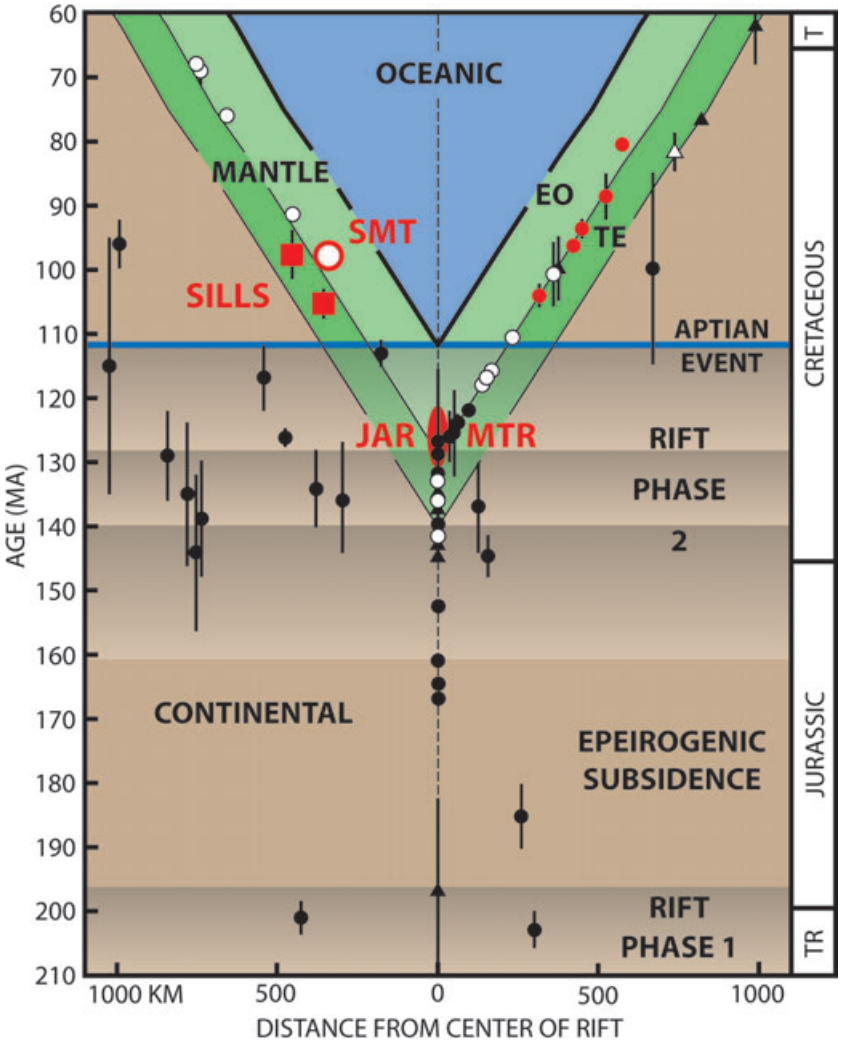

Figure 2. Summary of magmatism in space and time across the Newfoundland–Iberia rift, based on the compilation of age dates in Tucholke and Sibuet (2007) with added dates from Geldmacher *et al.* (2006), Merle *et al.* (2006); Grange *et al.* (2008). The North American Plate is on the left and the Iberia plate is on the right. Coloured fields show the distribution of basement domains through time with respect to the centre of the rift: continental (tan), exhumed mantle [green, 'transitional extension' (TE) and 'embryonic oceanic' (EO) domains], and oceanic (blue). Shading indicates rift phase 1 and rift phase 2 which included three episodes. The Aptian event (blue line) is interpreted to mark the first 'normal' oceanic crust. Black symbols with error bars are radiometric ages obtained on minerals with high blocking temperatures; these are considered to be reliable indicators of times of magmatism (see discussion in Tucholke & Sibuet, 2007). Open symbols show dates on plagioclases, which have blocking temperatures below ∼250 °C; these ages may have been affected by late-stage hydrothermal activity and may not reliably date times of primary magmatic activity. Triangles show samples from Gorringe Bank and a basalt sample (100 ± 5 Ma) from the northern perimeter of Galicia Bank. The former samples may represent igneous activity and/or re-setting of ages associated with post-rift tectonism at the Eurasia-Africa Plate boundary; thus, their relationship, if any, to rifting between Newfoundland and Iberia is uncertain. The red oval at the centre indicates magmatism that initially formed the J Anomaly Ridge, Southeast Newfoundland Ridge and Madeira-Tore Rise (collectively, JAR–MTR) at the rift axis near the southern margin of the rift; red dots show dated volcanics emplaced later at the MTR (Geldmacher *et al.* 2006; Merle *et al.* 2006). Post-rift sills drilled at ODP Site 1276 in the Newfoundland Basin are shown by red squares (Hart & Blusztajn 2006). A single plagioclase age date for one of the Newfoundland Seamounts (SMT) is indicated by the red circle (Sullivan & Keen 1977).

Aptian time (Aptian event, Fig. 2) when mantle exhumation is interpreted to have been replaced by relatively normal seafloor spreading (Tucholke *et al.* 2007). Afterwards, with minor exceptions in continental crust and at Gorringe Bank, all post-rift intrusions in basement are dated on plagioclases, which have blocking temperatures of less than ∼250°C (open symbols, Fig. 2). It is unclear whether these low-temperature dates indicate widespread post-rift, intra-plate magmatism or whether they record late hydrothermal circulation driven by residual heat from deep in the transitional lithosphere (Jagoutz *et al.* 2007).

The only clear evidence for significant post-rift magmatism occurs in the Newfoundland Basin at ODP Site 1276 (two diabase sills) and in the Newfoundland Seamounts (Fig. 1, and SMT in Fig. 2). The Site 1276 sills were penetrated less than 200 m above basement. The shallower sill is 10 m thick and lies at 1612.7–1623 mbsf. The deeper sill is at least 17 m thick and extends from 1719.2 m to 1736.9 mbsf; its full thickness is unknown because drilling was terminated due to poor penetration rates and hole-closure problems (Tucholke *et al.* 2004). The two sills are separated by 96 m of sediments, including a ∼10-m-thick undercompacted zone that has very low velocities (<1.7 km s^{-1}) and densities (<2.05 g cm^{-3}) near the bottom of the interval. The shallower sill was emplaced at ∼105.3 Ma and the deeper sill was emplaced at ∼97.8 Ma (^{40}Ar/^{39}Ar whole-rock ages; Hart & Blusztajn 2006). The sills are

hawaiites enriched in incompatible elements, which is suggestive of a mantle plume source (Hart & Blusztajn 2006). The ages of the sills are close to the apparent age of Scruncheon Seamount within the Newfoundland Seamounts about 190 km south of Site 1276. An age date obtained there by $^{40}Ar/^{39}Ar$ dating of plagioclase in a dredged trachyte is 97.7±1.5 Ma (Sullivan & Keen 1977).

The cause of the post-rift magmatism in the Newfoundland Basin is uncertain. The main competing hypotheses invoke passage of the lithosphere over one or more mantle plumes (Duncan 1984; Karner & Shillington 2005) or the reactivation of fracture zones (Pe-Piper *et al.* 1994). As we will show later, sill magmatism associated with the U reflection occurs within a well defined zone in relation to regional basement depth and apparent basement type within the deep Newfoundland Basin, which leads us to consider a third hypothesis of tectonomagmatic asymmetry.

In the following, we describe the character and extent of the sills in relation to basement characteristics along the Newfoundland margin. We use this information, together with other documented magmatic history and observations from the conjugate Iberia margin, to evaluate possible magma sources.

3 BASEMENT STRUCTURE

3.1 Basement seismic mapping: method

We interpreted the top of basement in the MCS profiles and mapped it across the margin from the Grand Banks basins seaward into the deep Newfoundland basin (Fig. 3). In some deep-basin areas, sills at the level of the U reflection mask the underlying basement, and it is not possible confidently to identify the basement surface. In these cases we estimated the top of basement to be the deepest reflection that has an amplitude equal to at least 50 per cent of the amplitude of the overlying U reflection (e.g. dotted line, Fig. 4b). As has been shown at Site 1276, a high-amplitude reflection also occurs below U in some areas and it probably correlates with a deeper sill (Shillington *et al.* 2007); in these areas the 50 per cent criterion was applied with respect to this deeper reflection. The 50 per cent threshold was estimated based on synthetic seismograms, as described in Section 5.

3.2 Basement seismic mapping: results

Based on our analysis and the published literature (Funck *et al.* 2003; Hopper *et al.* 2004, 2006; Lau *et al.* 2006a,b; Shillington *et al.* 2006; Van Avendonk *et al.* 2006, 2009; Tucholke *et al.* 2007), we define three basement domains (continental, transitional and embryonic oceanic) on the basis of seismic character (Fig. 3; see also Fig. 9). A fully oceanic domain farther seaward is not discussed here.

The *continental domain* occurs in the western and northwestern parts of the study region, that is across the Grand Banks shelf, Flemish Cap, and continental slope, and it extends eastward under the continental rise at least to the seaward flank of the 'H-block' (Figs 1b, 3, 4a and 9). The H-block, as defined by Lavier & Manatschal (2006), is a thinned continental block isolated near the seaward edge of continental crust by tectonic extension. Following the Peron-Pinvidic & Manatschal (2009) interpretation of SCREECH 2, we identify a block comparable to the H-block on SCREECH lines 1 and 3 (e.g. Figs 4a and 9), where seismic refraction data indicate that crustal thickness is about 6–10 km (Funck *et al.* 2003; Lau *et al.* 2006b; Van Avendonk *et al.* 2006, 2009). The continental basement at and landward of this block is commonly internally reflective, shows a relatively well-defined top limit, and is capped by variable thicknesses of pre-, syn- and post-rift sediments; the pre-/syn-tectonic sediments are regularly tilted over the fault blocks (Hopper *et al.*, 2004; Lau *et al.*, 2006a; Shillington *et al.*, 2006). Refraction data show that the continental crust thins abruptly seaward through the outer limit of the H-block, typically being reduced in thickness from >30 to <5 km in less than 100 km (Funck *et al.* 2003; Lau *et al.* 2006b; Van Avendonk *et al.* 2006). The refraction studies of Lau *et al.* (2006b); Van Avendonk *et al.* (2006) also suggest that allochthonous blocks of continental crust less than ∼5 km thick may extend for distances of tens of kilometres seaward of the H block.

East of the continental basement is a domain of *transitional basement*. It extends seaward ≥200 km at and south of SCREECH 3, but it narrows northward to ∼80 km at SCREECH 2 and either pinches out or is very narrow (∼10 km) at SCREECH 1 (Fig. 9) (this zone corresponds to transitional domain TE1 of Tucholke *et al.*, 2007). Its seaward limit lies near anomaly M3/M4 at the Hauterivian–Barremian boundary and is marked by a pronounced change from limited basement roughness to higher-amplitude topography farther east (Figs 3a and 4a). Reflectivity of the basement is variable. There is no distinct top–basement boundary along SCREECH 2 (Fig. 4) and the eastern part of SCREECH 3, and in these areas the true roughness of the basement is uncertain. Such weak basement reflectivity is usually observed where there is an overlying sequence of strong reflections (likely sills) associated with the U reflection. Shillington *et al.* (2008) used complex trace analysis to show that the weak reflectivity can be explained by poor signal penetration. Along the western part of SCREECH 3 (Fig. 5), and in some parts of the basin farther to the south, the basement surface and accompanying sedimentary onlap are better defined and internal basement structure is observed.

The nature of the transitional basement is still debated, but most investigations suggest that it is predominantly serpentinized mantle. Refraction data from both the Newfoundland and Iberia margins show velocities in the <5 to >7 km s^{-1} range as well as velocity gradients that appear to be best explained by serpentinization that decreases with depth into basement (Chian *et al.* 1999; Dean *et al.* 2000; Funck *et al.* 2003; Lau *et al.* 2006b, Van Avendonk *et al.* 2006). ODP Sites 897 and 899 on the Iberia margin recovered serpentinized peridotites in the conjugate transition zone (Sawyer *et al.* 1994). Magnetic anomalies over transitional basement have low amplitudes and poor continuity, and this has been interpreted as evidence for the presence of serpentinized mantle (Sibuet *et al.* 2007), although the basement also may contain discrete magmatic intrusions (Whitmarsh *et al.* 2001; Russell & Whitmarsh 2003). We place the western boundary of the transitional domain at the seaward edge of the H-block (Fig. 9); thus, the western part of this domain may include thin continental crust, as noted earlier.

Farther seaward, the *embryonic oceanic domain* lies between anomaly ∼M3/M4 and basement at the ∼Aptian–Albian boundary within the Cretaceous magnetic quiet zone (Figs 3 and 9) (this domain is the same as transitional extension zone TE2 of Tucholke *et al.*, 2007). The seaward boundary correlates in time with the Aptian event that has been interpreted to mark the onset of normal seafloor spreading (Tucholke & Sibuet 2007; Tucholke *et al.* 2007). The domain is <100 to >160 km wide on both the Newfoundland and Iberia margins. Embryonic oceanic basement has significantly higher-amplitude roughness than the transitional basement, with up to 1–1.5 km relief (Figs 3a and 4a—right side). Magnetic anomalies

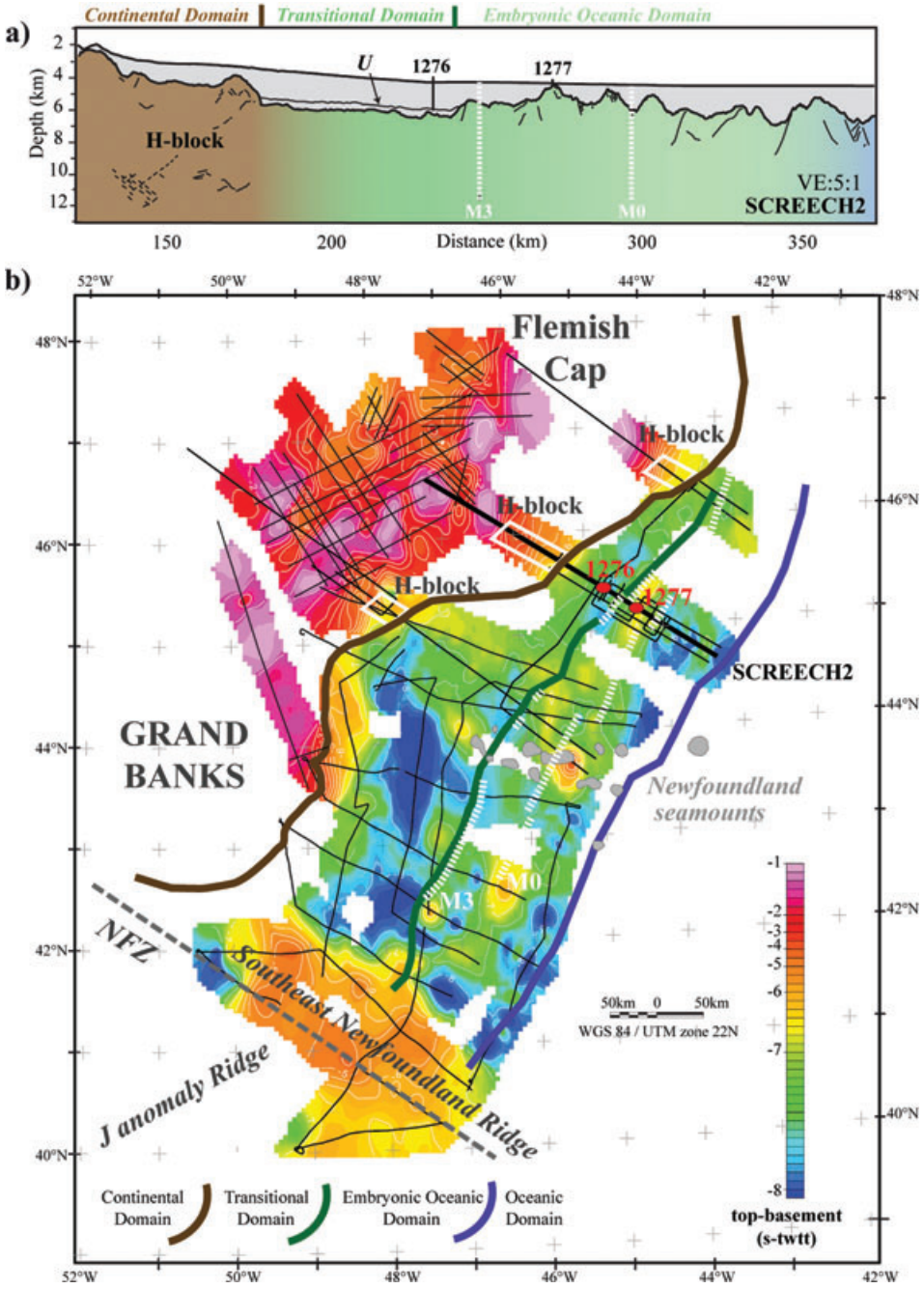

Figure 3. Contour map of basement depth (seconds two-way traveltime, s-twtt) across the Newfoundland Basin and adjacent shallower margin. Gridding method: kriging (Oasis Montaj; Journel & Huijbregts 1978). Contour interval is 0.5 s. Magnetic anomalies M3 and M0, basement domains (continental, transitional and embryonic oceanic) and ODP Sites 1276 and 1277 are indicated. The insert at top is a simplified interpretation of the SCREECH 2 reflection profile that shows basement domains discussed in the text (adapted from Shillington *et al.* 2006).

also are better developed than in the transitional domain, although the strong development of at least the younger anomalies (M1–M0) probably reflects plume influence in formation of the 'J' magnetic anomaly, as previously noted. Seismic characteristics of the basement are variable. In some places the upper 0.5 km of basement exhibits strong, chaotic reflections, whereas in other places more coherent, stratified reflections are observed. Lau *et al.* (2006a); Shillington *et al.* (2006) interpreted these features as arising from variable porosity in volcanic rocks and serpentinized mantle, but the actual composition of this basement remains controversial. Interpretations of velocity structure on various refraction profiles across the Newfoundland and Iberia margins span the gamut of possible compositions, ranging from thin oceanic crust over either normal or strongly serpentinized mantle, to normal oceanic crust, to mixed oceanic and serpentinite, to distinct zones of normal oceanic crust and serpentinized mantle (Whitmarsh *et al.* 1996; Chian *et al.* 1999; Dean *et al.* 2000; Funck *et al.* 2003; Lau *et al.* 2006b; Van Avendonk *et al.* 2006; Afilhado *et al.* 2008). The only direct evidence for composition of the basement is from three ODP drill sites (637, 1070, 1277), each of which sampled predominantly serpentinized peridotite, with or without minor mafic igneous rocks (Boillot *et al.* 1987a; Whitmarsh *et al.* 1998; Tucholke *et al.* 2004);

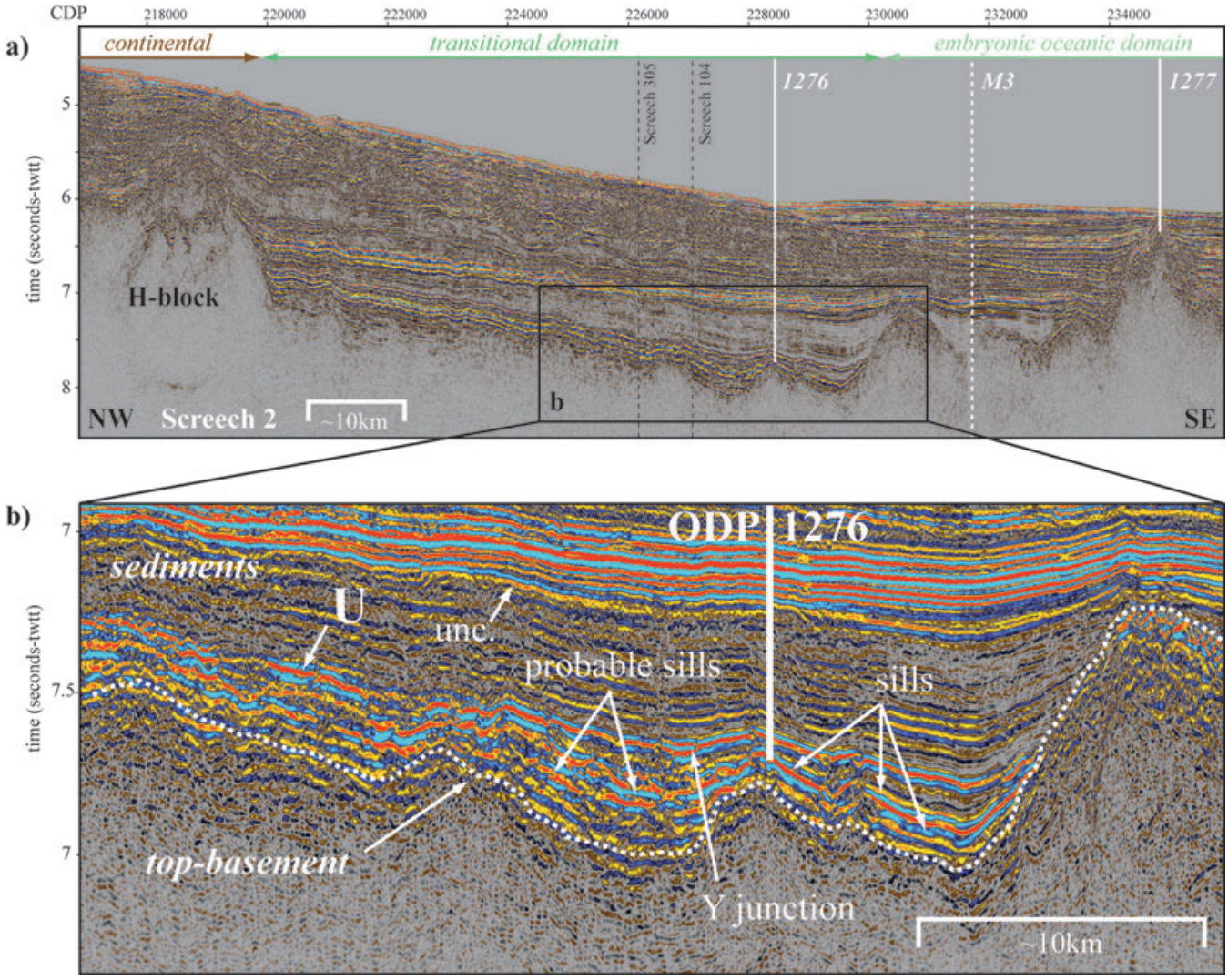

Figure 4. (a) Segment of MCS reflection profile SCREECH 2 (Shillington *et al.* 2004) which crosses ODP Sites 1276 and 1277. Location in Fig. 1. Basement domains and magnetic anomaly M3 are indicated. Vertical exaggeration is ~13 at the seafloor. (b) Enlargement of the SCREECH 2 profile across Site 1276, which penetrated two diabase sills. Dotted line shows approximate minimum basement depth, based on reflection amplitudes as described in text. The U reflection, an unconformity (unc.) in the overlying Turonian–Campanian sedimentary section, and 'Y' junctions in sills are indicated. Colours of reflections indicate relative amplitude of reflection peaks and troughs (warmer and cooler colours, respectively).

the latter two drill sites sampled basement that refraction velocity models would suggest is oceanic crust. Considering all these results, much of the embryonic oceanic domain may be exhumed, serpentinized mantle, although it may include localized and spatially variable components of mafic igneous intrusions and volcanic rocks; if such igneous rocks are present in substantial quantities, they could reflect a magmatic component that increased with time and led into normal seafloor spreading.

4 SILLS ASSOCIATED WITH THE U REFLECTION

4.1 Sills seismic mapping: method

We used MCS data to map the character and distribution of sills associated with the U reflection in the Newfoundland Basin. As already noted, U in the deep Newfoundland Basin generally is a high-amplitude reflection that correlates to the upper of two diabase sills where drilled at ODP Site 1276 (Tucholke *et al.* 1989; Shillington *et al.* 2007, 2008). However, it is not necessarily true that all strong reflections in the sedimentary sequence correspond to intrusions. To optimize our interpretations, we used the criteria of Planke *et al.* (2005) to identify a seismic event as an intrusion. First, a reflection was considered to be a possible sill if it is a high-amplitude event. Then, if the reflection also satisfies additional criteria, we interpreted it as a sill. Our criteria for identifying sills are summarized later.

4.1.1 Amplitude

The strong impedance (density × velocity) contrast between sedimentary and igneous rock generates a high reflection coefficient (> ~0.25), so sill reflections generally have high amplitudes. For example, Shillington *et al.* (2008) estimated a reflection coefficient of 0.337 for the top of the upper sill at Site 1276 based on measured density and velocity of core samples there. However, sill thickness

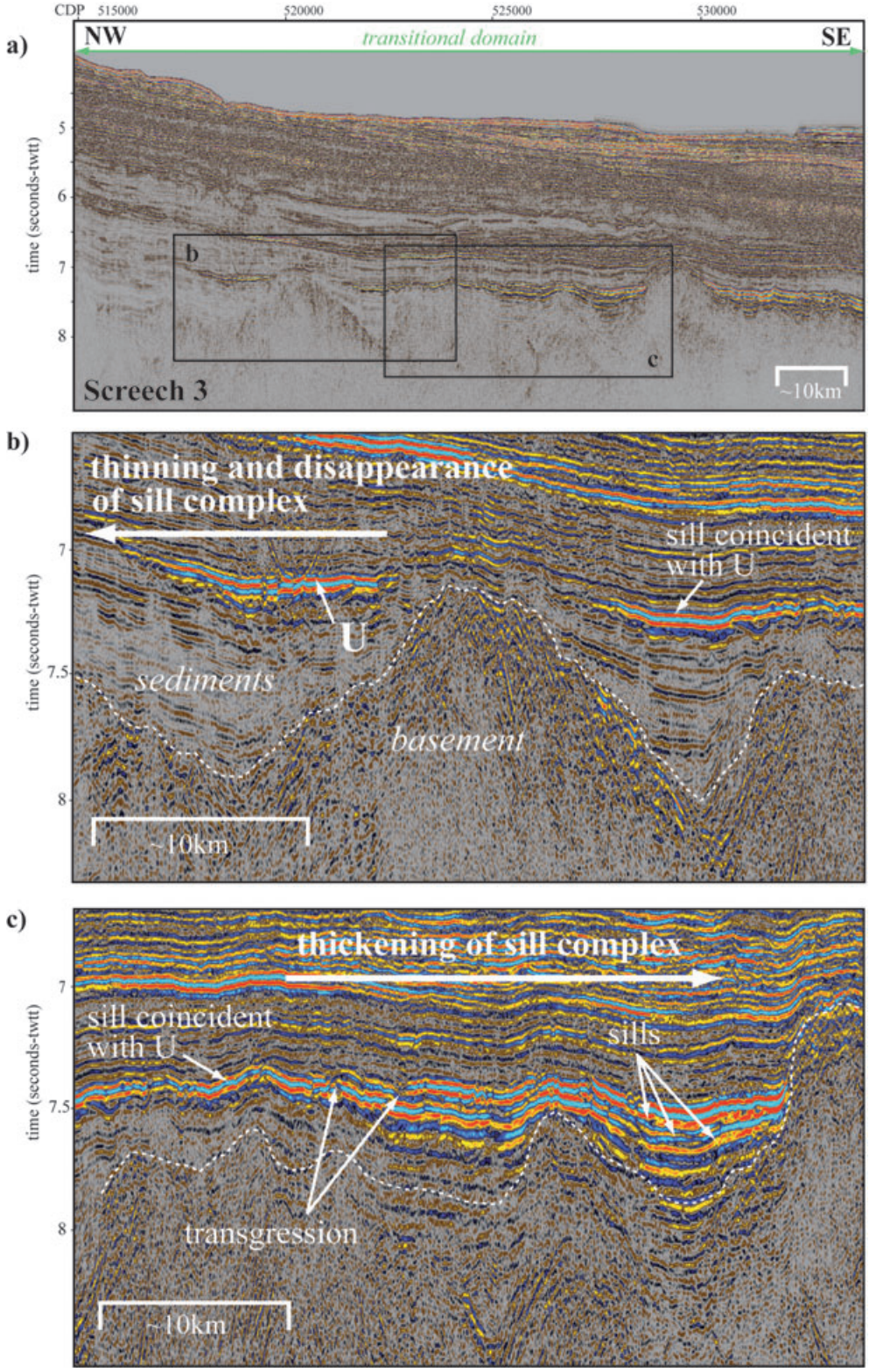

Figure 5. (a) Segment of MCS reflection profile SCREECH 3 (Lau *et al.* 2006a). Location in Fig. 1. Although we treat this as transition-zone basement, we note that Lau *et al.* (2006a) interpret basement out to CDP 528000 as very thin continental crust. Vertical exaggeration is ~13 at the seafloor. (b,c) Enlargements showing details of sill structure and sedimentary stratigraphy. Explanation as in Fig. 4.

also exerts control on seismic amplitude due to destructive or constructive interference of reflections from the top and the base of the sill (e.g. Widess 1973). Studies on volcanic margins show that some sills are sufficiently thick (~150 m) to generate distinct reflections from upper and lower contacts for the dominant frequencies in deep-penetration reflection data (~10–50 Hz); however, most intrusions are thinner (~50–100 m) and this prevents mapping the lower sill boundaries (Hansen & Cartwright 2006; Planke *et al.* 2005). Using

the SCREECH data, we explored the consequences of sill thickness for seismic amplitude and characteristics by creating synthetic seismograms (Section 5).

The academic and industry MCS data used in this study were recorded and processed using a variety of acquisition systems and processing parameters. Thus, it is not possible to compare reflection amplitudes directly among all profiles. However, high-amplitude reflections within any profile can be identified by comparing them with immediately surrounding reflections and with reflections that are at the same subbottom depth elsewhere in the record, irrespective of the acquisition/processing parameters (e.g. automatic gain control). We used this criterion to identify reflections of unusually high amplitude.

4.1.2 Structure

Sill intrusions are associated with a variety of characteristic structural and stratigraphic features (Thomson & Hutton 2004; Planke *et al.* 2005). Many of these are present in the deep Newfoundland Basin in forms that range from well developed to poorly developed, as summarized later.

Sill transgression occurs where a sill reflection cuts up through successive layers of sedimentary strata. Although we observe this phenomenon in the basin, it is relatively rare and it reaches over only short stratigraphic intervals (Fig. 5c). Almost all the sills that we identify occur at one stratigraphic level, that is at the U reflection (Figs 6b–c, 7 and 8) or are confined below that level. Sills at the

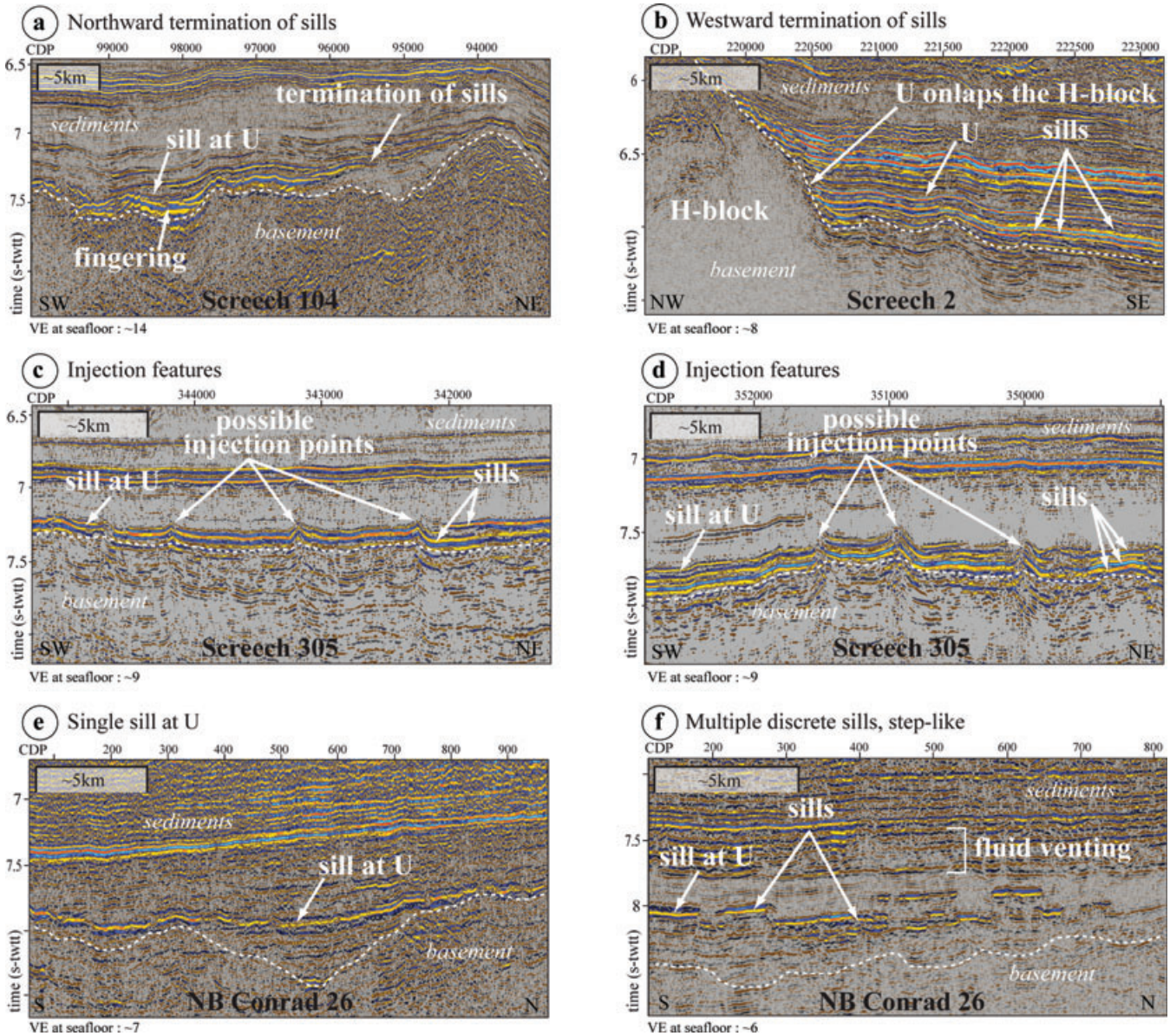

Figure 6. Segments of MCS reflection profiles illustrating sill features over transitional basement. Explanation as in Fig. 4, and locations in Fig. 1. (a) SCREECH 104 (Shillington *et al.* 2004), near the northward pinchout of the U reflection. (b) SCREECH 2 (Shillington *et al.* 2004), showing westward pinchout of U on the H-block, and interpreted sills below U. (c,d) SCREECH 305 (Deemer *et al.* 2009) in the north central basin; single and multiple sills are relatively flat except for local highs that may be locations of dike/pipe injection around which the sills later subsided due to compaction of underlying sediments. (e) Conrad profile NB 26 (Tucholke *et al.* 1989) in the central basin south of the Newfoundland Seamounts; intrusion of a single sill at the level of the U reflection is common in this area. (f) Conrad profile NB26 (Tucholke *et al.* 1989) in the southern basin, showing discrete, step-like sills injected at or near the U reflection; sills with this character are restricted almost entirely to the southern Newfoundland Basin.

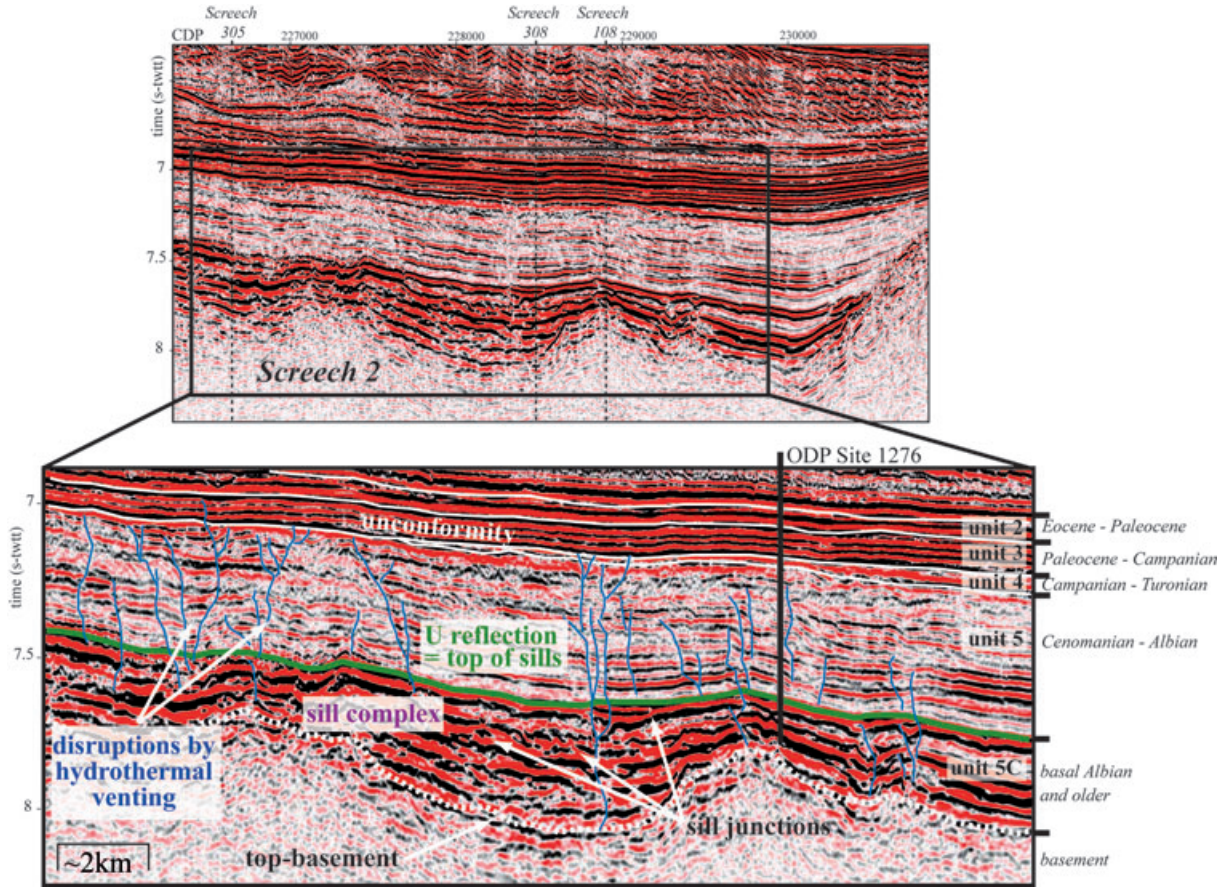

Figure 7. Segment of SCREECH 2 MCS profile through ODP Site 1276 (Shillington *et al.* 2004). Red and black indicate amplitude peaks and troughs, respectively. Vertical exaggeration is ∼9 at the seafloor. The expanded section at bottom shows lithologic units defined at Site 1276 (Tucholke *et al.* 2004), and the white dotted line indicates minimum basement depth as described in the text. The upper sill drilled at Site 1276 is coincident with the U reflection. Disruptions in lithologic Unit 5 are interpreted as pathways of hydrothermal venting associated with sill injection. Note that there is little such disruption in overlying lithologic units and that Unit 4 is attenuated and in some places removed by erosion (e.g. at left in bottom panel). See text for discussion.

level of U are remarkably continuous over distances of tens of kilometres and more. Following Francis (1982), Tucholke *et al.* (2004) suggested that this restricted upper limit of intrusion is explained by the magma reaching a level of hydrostatic equilibrium at a shallow subbottom depth and then flowing laterally with little frictional resistance, much like subaerial flood basalts. Such layer-parallel intrusions are expected in unconsolidated sediments without any elastic strength (Planke *et al.* 2005). The only significant exceptions to this upper limit are observed in the southern part of the basin, where short sill segments appear up to ∼200 ms two-way traveltime above U (Fig. 6f). These sills do not cut across sedimentary strata as a transgressive phenomenon. Instead they have 'step-like' form and abrupt terminations; both kinds of features are characteristic of sills.

Other observed sill features include junctions (wherein a sill splits in a 'Y' geometry; Fig. 4b) and finger-like structures (wherein subparallel sill segments form a series of separate bodies in an en-echelon pattern; Fig. 6a). These and other kinds of disruptions occur predominantly in the section below the more continuous sills at the U reflection. Sill reflections generally mimic the underlying basement topography by following layering in the compacted sediments (e.g. Figs 4 and 6), which demonstrates that bedding exerted strong control on magma injection. Interestingly, we observed no instances of saucer-shaped sills, which globally are a common phenomenon (e.g. Planke *et al.* 2005).

One of the most common sill-related features in the Newfoundland Basin is perturbation of the sedimentary section overlying the U reflection (e.g. Figs 6a,d,f and 7b). In this section, there is often strong variation in both the continuity and amplitude of reflections, probably because of the effects of fluid venting associated with sill emplacement.

Finally, as noted earlier, where sills are present there is widespread amplitude blanking of basement reflections because of signal attenuation (Shillington *et al.* 2008).

4.2 Sills seismic mapping: results

4.2.1 Geographic distribution of sills

Features that are interpreted as sills cover an area of ∼80 000 km^2 (∼820 km SW–NE and between ∼50 and ∼200 km NW–SE). They are restricted to the area of the transitional domain (Figs 9 and 10) and thus overlie the deepest basement in the Newfoundland Basin (Fig. 14). Towards the northwest, the sills stop at the H-block (SCREECH 2, Figs 4 and 6b) or gradually disappear westward at the level of the U reflection before reaching this block (SCREECH 3, Fig. 5a). Towards the northeast the sills terminate in sediments immediately above the shoaling basement near Flemish Cap (SCREECH 104, Fig. 6a). To the east and south, the sills terminate against pronounced blocks of embryonic oceanic crust near

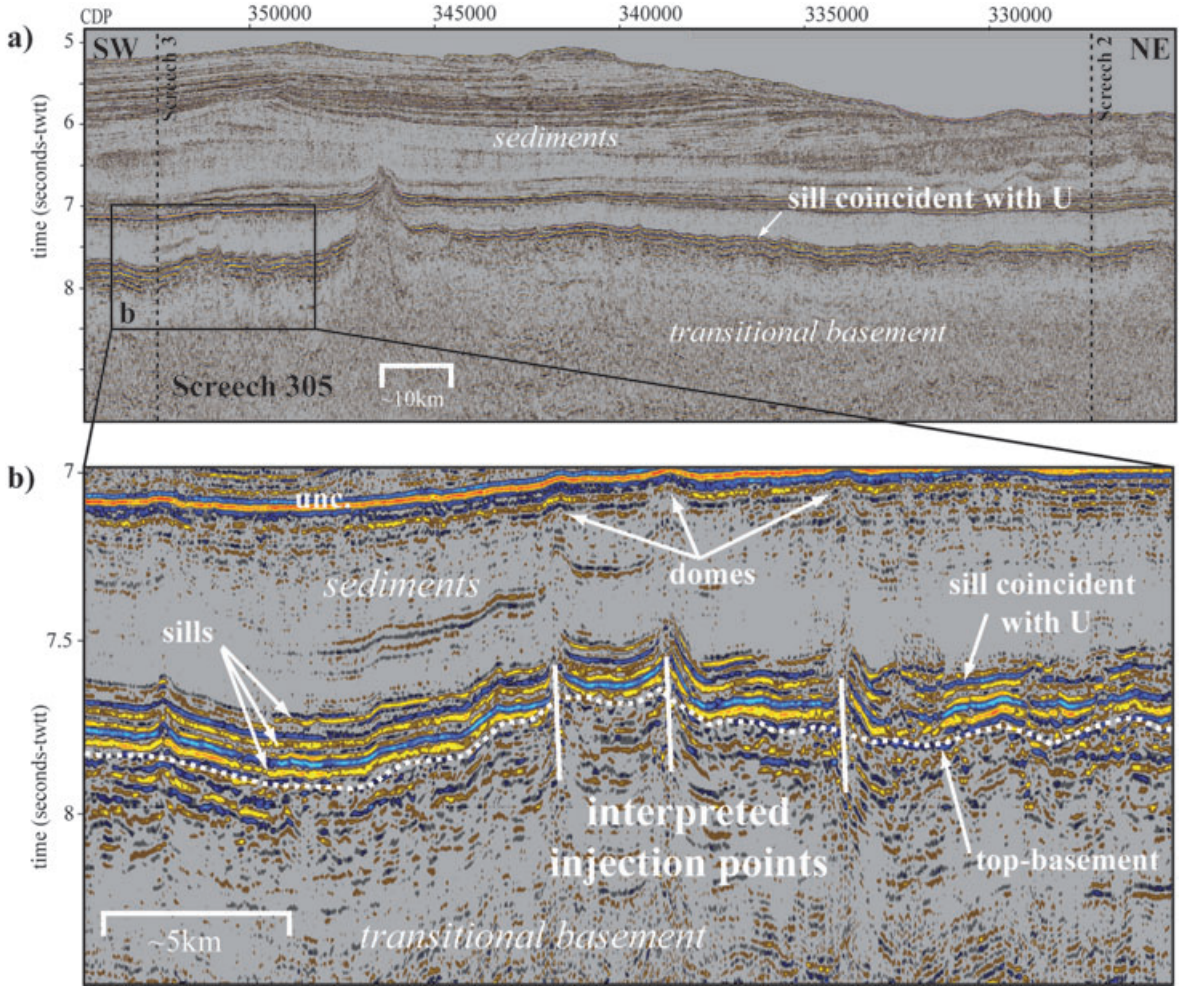

Figure 8. (a) Segment of MCS reflection profile SCREECH 305 (Deemer *et al.* 2009). (b) Enlargement showing details of sill structure and sedimentary stratigraphy. Explanation as in Fig. 4 and location in Fig. 1. Peaks in the sills are interpreted as possible magma injection features (dikes or pipes) that solidified and remained high while the surrounding sills subsided during sediment compaction. Vertical exaggeration is ~15 at the seafloor.

anomaly ~M3 (Fig. 4a) and against the Southeast Newfoundland Ridge, respectively. Although sills are intimately associated with the U reflection across the transitional domain, this is not the case in areas outside the domain. The U reflection extends far beyond these bounds, reaching well onto Aptian basement to the east (e.g. Tucholke *et al.* 2007) and onto the Southeast Newfoundland Ridge and the Grand Banks shelf (Tucholke *et al.* 1989). In these areas we have not been able to identify any features that can confidently be associated with the presence of sills.

4.2.2 Distribution of sill-related features

Major patterns of sill reflection geometry and amplitude vary throughout the Newfoundland Basin. Subcontinuous, high-amplitude reflections with step-like geometries (Fig. 6f) occur only in the southern half of the basin. Many of these reflections extend for just a few kilometres (usually <1 to 4–5 km). It is unknown whether the sills were intruded during a single or multiple injection events. In this region there are some areas without strong reverberation in the sub-U section, as well as sufficient seismic signal penetration to image the underlying sedimentary sequence and top of basement. This suggests that there may be only limited occurrence of sills below the U reflection.

In contrast, in the region of SCREECH 3 to the north, short, step-like sill segments are mostly absent, and there is typically a strong, singular reflection at U that is more continuous (Figs 5 and 6c–e). Compared to the southern basin, the overlying sedimentary sequence also becomes more disrupted by apparent effects of fluid venting. The sequence below U commonly exhibits a thick interval of strong reflections with moderately good continuity, although there are small local disruptions and Y-like junctions of reflections. The degree to which this interval represents numerous sill intrusions, as opposed to seismic reverberation associated with the high-amplitude U reflection, is uncertain. The top of basement is locally hidden within this sequence and can be difficult to identify (e.g. Figs 6c and d). The poor imaging of basement probably indicates reduced signal penetration due to an increase in the frequency or thickness of sills as compared to the basin farther to the south.

Northward, in the area of SCREECH 2, reflection amplitudes at U remain high (Figs 4 and 8). The reflection is relatively continuous, although there are local finger-like structures, junctions, and abrupt endings. Disruptions in overlying strata that appear to be related to hydrothermal venting are common (e.g. Fig. 7). Reverberation in the underlying interval generally is very strong, so identification of basement is difficult.

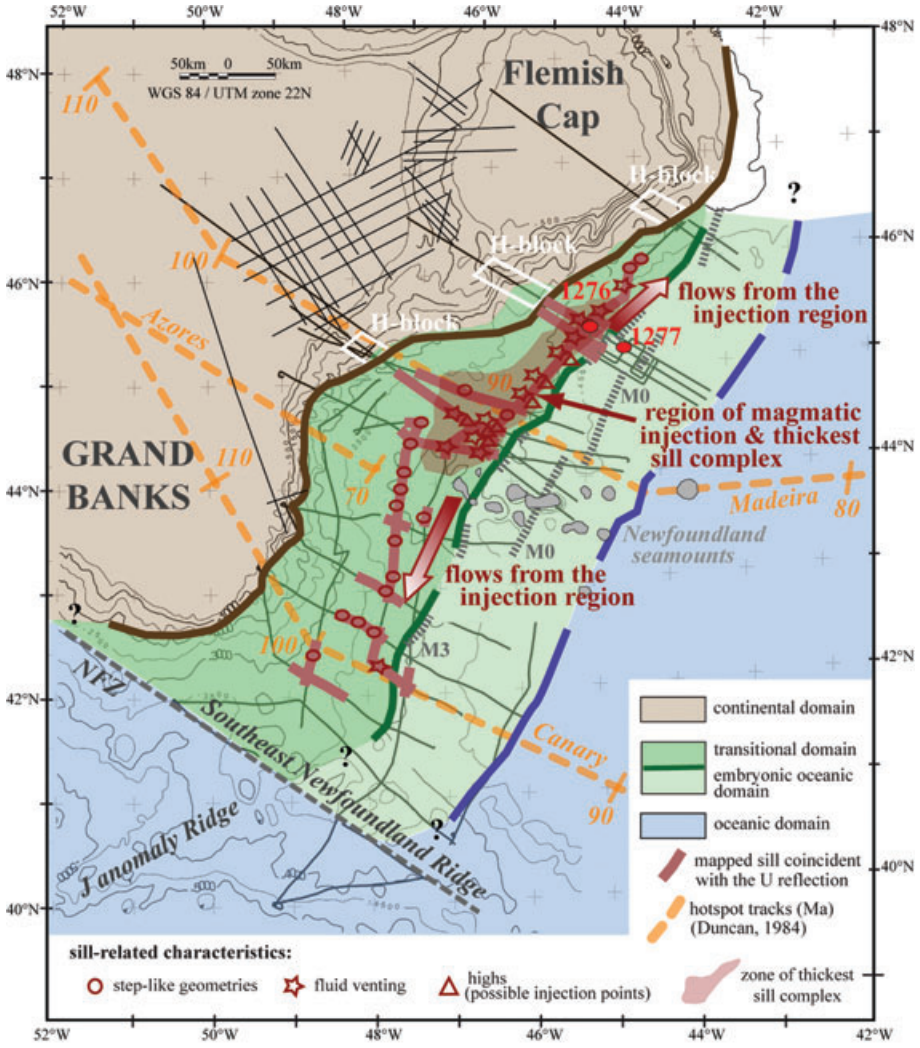

Figure 9. Map summary of basement types and distribution of post-rift igneous sills. Tracks of the Canary, Azores and Madeira plumes (Duncan 1984) are shown. Red bars along ship track lines show the distribution of mapped sills coincident with the U reflection. The light red shading within the transitional domain shows where the sill complex is thickest; this area is considered to be the main locus of magma injection into post-rift sediments. As suggested by the arrows, magma may have been distributed away from this area within both the lithosphere and the sediments. Red symbols, identified in the legend at lower left, denote the general distribution of characteristic sill features in the basin.

Where the high-amplitude reflection at U is relatively flat in the area of both SCREECH 2 and 3, we commonly observe local 'highs' in the reflection (Figs 6c,d and 8b). Some of these may overlie basement peaks. Another possibility is that they mark locations of underlying dikes or pipes where magma was injected. In either case, it appears likely that the highs represent points where the sill is supported by rigid deeper structure, and between these points the sill sagged and became deeper as overburden increased and the underlying sediments were compacted (Section 6.3).

In the area north of SCREECH 2, basement shoals and the U reflection pinches out in the overlying sediments (Fig. 6a). High amplitudes are associated with sills both at the U reflection and in the sub-U sequence. All these reflections are less continuous than they are to the south. They tend to follow the shape of the immediately underlying basement and are locally disrupted by basement peaks. No step-like geometries are observed, but reflections in overlying sediments are disrupted by apparent fluid venting.

Overall, the distribution of various sill-related features suggests that there was a centre of magmatic activity located in the region of the SCREECH 3 profile and extending north to the area of SCREECH 2 (Fig. 9). This central region is characterized by strong, relatively continuous sill reflections, local highs that were possible loci of magma injection and common fluid venting features in the overlying sediments. It also contains the thickest high-reflectivity sequence in the sub-U interval, suggesting that it is closest to the source. To the north and south of this zone, the sub-U sill sequence is thinner, and the sills at U have lower reflectivity and/or tend to be less continuous.

4.2.3 Fluid venting associated with sill emplacement

We interpret common disruptions of the sedimentary sequence above the U reflection to be related to fluid venting associated with sill emplacement, as illustrated on the SCREECH 2 profile through ODP Site 1276 (Fig. 7). The disruptions appear as subvertical, possibly branching zones where normal reflectivity of bedding is strongly attenuated, where the layering is disrupted or contorted, or both. Similar hydrothermal features have been described as

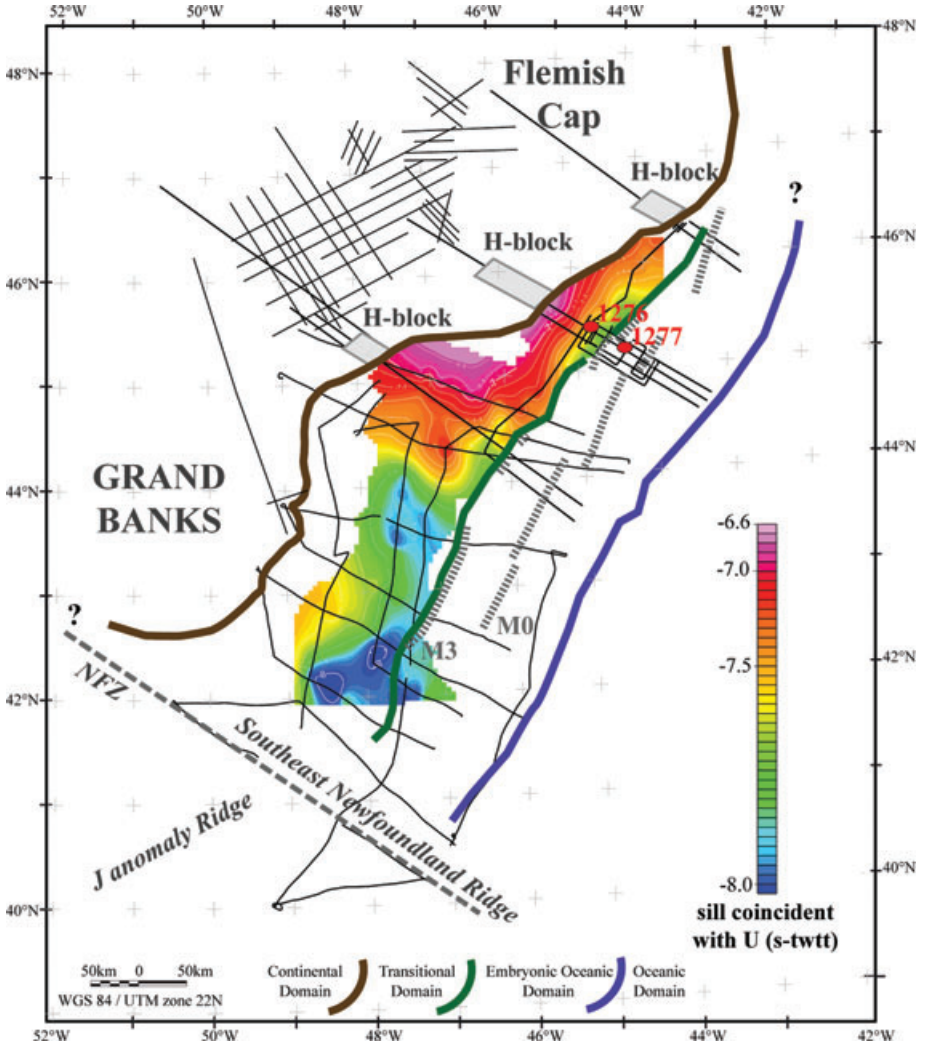

Figure 10. Structure contour map on the top of sills at the U reflection in seconds two-way travel time (s-twtt). Gridding and display are as noted for Fig. 3. Contour interval is 0.1 s. Basement domains, magnetic anomalies M3 and M0, and ODP Sites 1276 and 1277 are indicated.

sill-related structures in other areas (Planke *et al.* 2005; Hansen & Cartwright 2006). The disrupted zones often, but not always, correlate with interruptions or local highs in the upper sill at the U reflection (Fig. 7), and these may have been preferred sites for fluid escape into the overlying sediments. Correlative disruptions in the strong reflections below U are sometimes observed, suggesting that fluids venting from sub-U intrusions may have caused breaching of the upper sill in some places.

At ODP Site 1276, disruptions associated with venting affect all of lithologic Unit 5 (Fig. 7). This unit is 516 m thick above the upper sill and consists largely of black shales dating from early Albian to middle Turonian (∼112 to ∼92 Ma; Tucholke *et al.* 2004). Overlying sediments of lithologic Units 4 (Turonian–Campanian reddish-brown sandstones and mudstones) and shallower units show little or no disruption by venting. Unit 4 contains either unconformities or intervals of extremely slow deposition and is barren of calcareous microfossils (Urquhart *et al.* 2007). The duration of the missing interval(s) is uncertain but could be as much as ∼10 Myr, so the base of Unit 4 could be anywhere from ∼92 to ∼82 Myr old. Thus, the period over which hydrothermal venting was active was a minimum of ∼6 Myr, that is from the time of ∼98 Ma injection of the younger sill until ∼92 Ma. The maximum duration of venting was ∼23 Myr, that is from the time of injection of the older sill (∼105 Ma) until ∼82 Ma.

Planke *et al.* (2005) observed common crater, dome or 'eye' structures within sediments at the shallowest levels affected by hydrothermal venting on the Norwegian margin. We have not identified crater or 'eye' structures at the lithologic Unit 4/5 contact in the Newfoundland Basin, but if erosion was responsible for developing an unconformity at this contact it may have removed evidence of such features. There are some places where minor doming is observed at the contact and in the immediately overlying sediments (e.g. Fig. 8). This might indicate that venting continued to times even younger than ∼83 Ma, that is into Campanian time, although the doming could also be original depositional structure.

At ODP Site 1276, vitrinite reflectance and palynomorph data indicate that sediments experienced thermal alteration only within 20 m of the upper sill and that alteration decreases substantially more than 4 m away from the sill (Pross *et al.* 2007). This would seem to contradict our interpretation that more than 500 m of overburden was affected by hydrothermal venting. However, the flow of hot fluids probably was restricted to relatively narrow channels, and there is no evidence that such a channel was penetrated at the drill site. Alteration at Site 1276 therefore appears to

represent only contact metamorphism that was associated with magma injection.

The earlier descriptions summarize the lateral distribution of sills and their characteristic features. However, aside from the strength of sub-U reflections that give some insight into the presence of deeper injections, these features provide little information about the vertical distribution of intrusions and thus the potential volume of post-rift magmas. In the next section, we constrain these parameters by using synthetic seismograms to investigate relations between reflection amplitude and sill thickness.

5 SYNTHETIC SEISMOGRAMS

5.1 Synthetic seismograms: method

We created a series of synthetic seismograms to explore variations in sill thickness and frequency that might be responsible for observed variations in seismic reflection characteristics in the SCREECH 2 MCS data, for which the acquisition and processing parameters are well known (Shillington *et al.* 2006, 2007). We used the reflectivity method to generate the seismograms (Kennett 1983), as implemented by the commercial package NUCLEUS [Petroleum Geo-Services (PGS)]. This method accounts for most aspects of the seismic wavefield that would be anticipated for a 1-D velocity structure, including interbed multiples and frequency-dependent effects of thin beds. These effects are not included in algorithms that produce synthetic seismograms by simple zero-offset convolution. To create synthetic seismograms, information on both the source wavelet and the velocities and densities of subsurface layers are required, and we summarize both of these inputs later.

Data from ODP Site 1276 constitute the only direct information available on subsurface properties of sediments and sills in the deep parts of the Newfoundland margin. Unfortunately, hole conditions prevented acquisition of logging data at the site, but an excellent suite of velocity and density data was obtained from the continuously cored hole. Shillington *et al.* (2007) used the vertical *P*-wave data and measured densities to create synthetic seismograms to link seismic and core data at the drill site (see 'Scenario 3' in Shillington *et al.* 2007), and we used those same data here. Vertical velocities were used because they most closely approximate the ray paths of reflections recorded in multichannel seismic reflection data. The velocity and density data were used to create an 'earth model', which consists of a series of layers with assigned *P*- and *S*-wave velocities, density and *P*- and *S*-wave attenuation (Q_P and Q_S, respectively). *S*-wave velocity was estimated from *P*-wave velocity (Castanga *et al.* 1986; Greenberg & Castagna 1992). We used a Q_P of 1000 and a Q_S of 5000 for water, 200 and 100 for sediments and 400 and 100 for sills (Fuchs & Müller 1971; Minshull & Singh 1993). We used the source wavelet of Shillington *et al.* (2007), which was estimated by modelling the far-field source signature produced by the airgun array used to acquire the SCREECH MCS data on R/V Maurice Ewing. Although we are concerned here only with the reflection attributes associated with sills in the deepest part of the sedimentary section, we include all available velocity/density information on the overlying sediments in our calculation because attenuation or interbed multiples caused by the shallower section can affect the appearance and amplitude of deeper features.

To explore the effects of sill thickness on the amplitude and character of seismic reflections, we calculated synthetic seismograms for a series of sill thicknesses as described in Section 5.2.3, but we left all other parameters (e.g. velocity) fixed.

5.2 Synthetic seismograms: results

5.2.1 Distinguishing reverberations from primary reflections

As described in Section 3, the top of basement is difficult to identify on some reflection profiles in the Newfoundland Basin. In these areas, a sequence of strong reflections is observed near the base of the sedimentary section, below the U reflection. We are confident that the uppermost reflections in this package arise from 'real' features due to their large associated amplitudes and lack of complete parallelism with overlying reflections. But it is unclear whether deeper reflections that parallel U represent reverberations or subsurface features. The most likely causes of reverberations are reflections that ricochet between layers of high impedance contrast in the subsurface (e.g. between the two sills encountered at Site 1276).

The reflectivity method used to generate synthetic seismograms includes such effects and thus can be used to assess the likely amplitude of reverberations. We compared the amplitudes of primary reflections and reverberations for all of the synthetic seismograms (Fig. 11), and we found that reverberations have amplitudes that are $\sim$34 per cent of primary reflections on average, with a maximum predicted reverberation amplitude of $\sim$40 per cent (for a 20-m-thick sill). Consequently, in areas that appear to have significant reverberations, we conservatively assumed (a) that any event with an amplitude $>$50 per cent of the overlying primaries is also a primary reflection, and (b) that the shallowest possible basement occurrence is where all reflections have amplitudes that are $<$50 per cent of the primaries.

5.2.2 Would there be a 'U reflection' without the presence of a sill?

To address this question, we calculated a synthetic seismogram using the laboratory measurements of velocity and density described earlier, but we omitted measurements associated with the upper sill (Fig. 12). With these omissions, physical property contrasts are small; thus, no strong reflection is predicted and only a couple of substantially weaker events are observed in the time interval of the U reflection. These events have significantly lower amplitude than the observed amplitude of U outside the area where sills clearly are present (Fig. 12). It may be that in the area of Site 1276 the sill intrusion obliterated sedimentary physical-property contrasts that are responsible for the U reflection in areas where sills are not present. Overall, however, our results are consistent with the idea that strong reflections at U are caused by sills and that U elsewhere in the deep basin is probably a much lower-amplitude event.

5.2.3 Effect of sill thickness on U reflection character

Based on results at ODP Site 1276 where the upper sill was only 10 m thick, it is clear that there are sills in the Newfoundland Basin that are too thin to generate distinct reflections from both their top and base. To assess the effect of sill thickness on seismic attributes, we calculated synthetic seismograms for sill thicknesses ranging from 5 up to 150 m (Fig. 11). This exercise demonstrates that amplitudes increase with increasing sill thickness until the thickness reaches $\sim$30 m, after which the amplitude decreases slightly and converges to a constant value (Fig. 11b). The maximum amplitude corresponds to the 'tuning thickness'; this is the smallest thickness where the actual sill thickness in two-way travel time equals the measured thickness between a peak associated with a positive polarity reflection marking the top of the sill and a trough

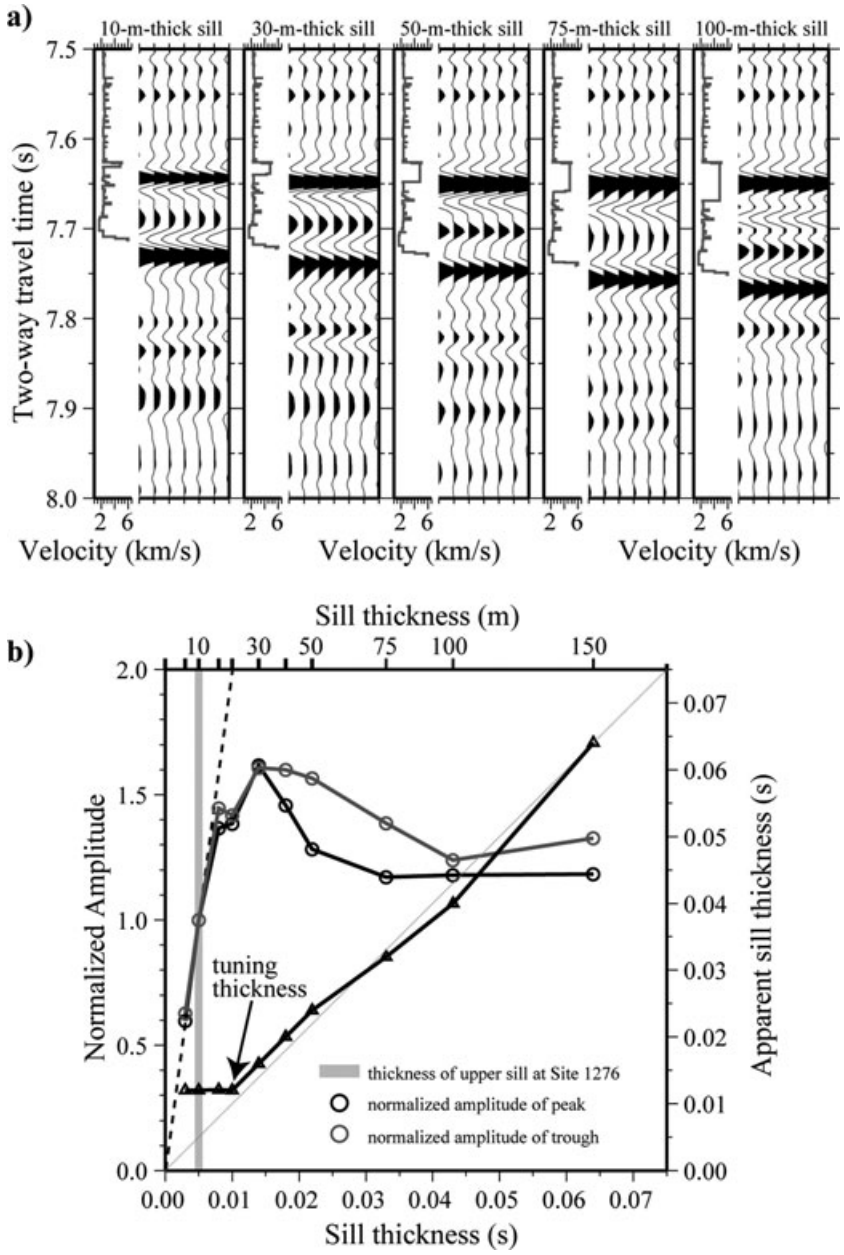

Figure 11. (a) Synthetic seismograms based on laboratory measurements of vertical *P*-wave velocity and density on cores from Site 1276 and assuming different thicknesses for the upper sill. All other aspects are held constant. For each synthetic seismogram, the velocity function is shown to the left and the resulting seismogram is shown to the right. The upper and lower sills are marked by high-amplitude events and are followed by lower-amplitude reverberations. The seismogram for a 10-m-thick sill is identical to the synthetic seismogram used to link core and seismic data by Shillington *et al.* (2007). (b) Normalized amplitude (circles) and apparent sill thickness (as measured in seconds two-way traveltime, triangles) versus actual sill thickness based on synthetic seismograms. Amplitude is normalized by the amplitude of the peak (black circles) and trough (grey circles) of a reflection associated with a 10-m-thick sill (as encountered at Site 1276). Note that the maximum amplitudes are predicted for a sill whose thickness is 30 m, the approximate 'tuning thickness' (Kallweit & Wood 1982). Amplitude then decreases and converges to a constant value for thicknesses greater than ∼75 m. For thicknesses ≥30 m, the actual thickness equals measured distance in two-way traveltime between a peak associated with the top of the sill and a trough associated with the base of the sill. For sill thicknesses <30 m, sill thickness can be estimated using reflection amplitude as described by Widess (1973) and illustrated with black dashed line. The thin grey dotted line shows apparent thickness = actual thickness for reference. Sill thicknesses expressed in seconds two-way traveltime assume a velocity of 4.4 km s^{-1} in the sill.

associated with a negative polarity reflection marking the base of the sill (Fig. 11b). At less than the tuning thickness, sill thickness can be estimated using seismic amplitude (Widess 1973; Kallweit & Wood 1982), as described later.

To estimate possible variations in thickness of the upper and lower sills, we applied a simple mapping strategy to the SCREECH 2 reflection profile. SCREECH 2 was chosen because it crosses Site 1276 and our estimates can be calibrated by drilling results there (Figs 4 and 7). The mapping strategy is described briefly here, and in detail by Kallweit & Wood (1982). Although many more sophisticated methods have been developed in the last 20 years for mapping thin beds using spectral methods (e.g. Marfut & Kirlin

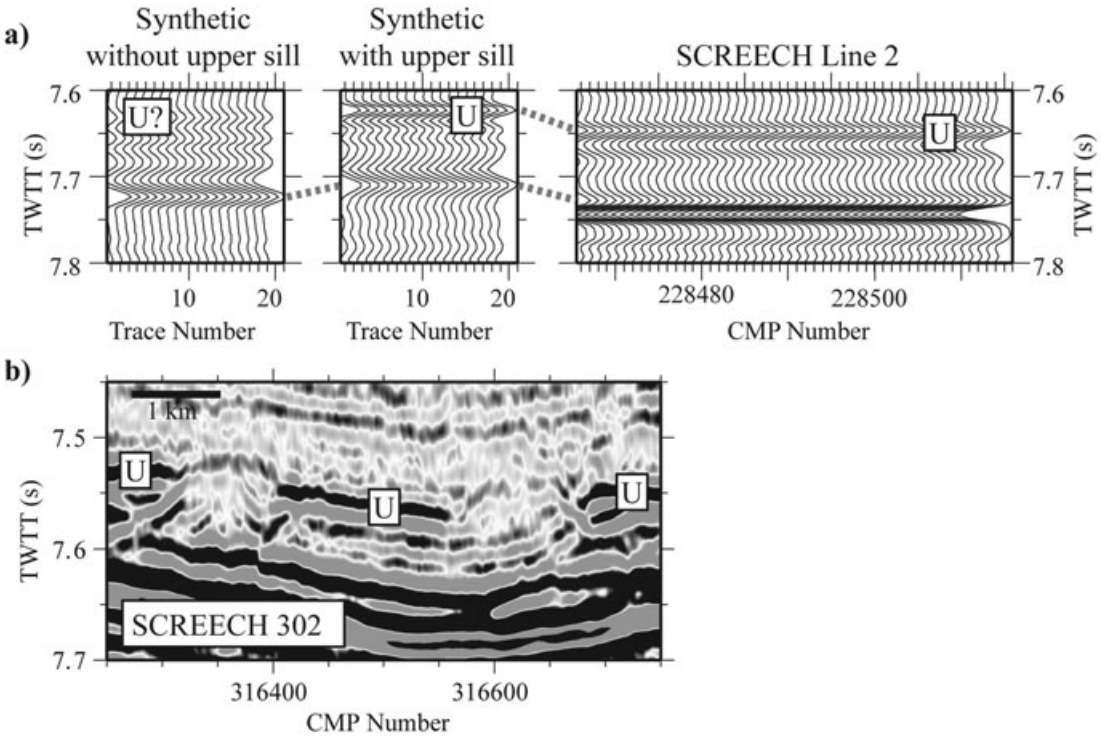

Figure 12. (a) Synthetic seismograms constructed using laboratory measurements of velocity and density from cores recovered at Site 1276 with (middle panel, after Shillington *et al.* (2007)) and without (left panel) the upper sill. Traces from SCREECH 2 at Site 1276 are shown at right. Note that a prominent reflection at the time interval of U is not predicted unless a sill is present. (b) Data example from SCREECH 302 showing abrupt lateral variations in amplitude at the level of the U reflection, which might be caused by sills with limited spatial extent; the profile is centred at 45.342°N 44.937°W and parallels the SCREECH 2 profile (Shillington *et al.* 2004).

2001; Puryear & Castanga 2008), we sought a simple approach that could be used to make first-order estimates of average sill thickness and thus to estimate the volume of magmatic material. The first step was to interpret a peak corresponding to the top of the sill and a trough corresponding to the base of the sill (Fig. 13a). For measured thicknesses greater than or equal to the tuning thickness (∼0.016 s), we estimated sill thickness by converting the measured thickness in two-way traveltime to actual thickness using a velocity of 4.4 km s^{-1} for the upper sill and a velocity of 5.87 km s^{-1} for the lower sill (average velocities of each sill are from shipboard laboratory measurements (Tucholke *et al.* 2004). For measured sill thicknesses less than the tuning thickness, we estimated the sill thickness using the approximate relationship presented by Widess (1973):

$$A_{\mathrm{d}} \approx 4\pi Ab/\tau V_{\mathrm{b}},$$

where A_{d} is the amplitude of the reflection, A is the amplitude to which thicker beds converge, b is the thickness of the bed, τ is the period and V_{b} is the seismic velocity of the bed. The predicted amplitude–thickness curve associated with this relationship, assuming a dominant frequency of 30 Hz and a velocity of 4.4 km s^{-1}, was calibrated using the amplitude characteristics associated with sills at Site 1276 and is shown by the black dashed line in Fig. 11(b). This relationship assumes that the impedance contrasts at the top and base of the bed are of identical magnitude but opposite sign. This assumption is justified based on the relatively linear relationship between the amplitudes of peaks and troughs associated with the top and base of each sill, respectively (e.g. Brown *et al.* 1986). The only amplitude correction that was applied to processed seismic data from which amplitudes were extracted was a spherical divergence correction (i.e. not AGC).

Variations in sill thickness along SCREECH 2 estimated from the earlier analysis are shown in Fig. 13b. Each of the sills appears to be ∼20–30 m thick along much of the line. Larger thicknesses of up to 100–150 m for each sill are estimated in some places, based on reflection amplitude and polarity (e.g. the upper sill at CMP 224000, inset in Fig. 13a). The average thickness of the upper sill is 48 m, and the average for the lower sill is 58 m. Overall, sills comprise an estimated ∼26 per cent of the depth interval between the sill at the U reflection and basement. These results are used to make a rough estimate of the volume of magmatic material in the discussion later.

6 DISCUSSION

6.1 Area and volume of magmatic rocks

The large area affected by sills (∼80 000 km^2), the evidence for at least two intrusions at Site 1276, and the common occurrence of strong sub-U reflections all suggest that a series of sills was intruded during multiple magmatic events. We hereafter refer to this series, up to and including strong reflections at or near the U reflection, as the 'sill complex'.

Widespread sill emplacements are known from other regions, so the large geographic extent of the sill complex is not exceptional. Planke *et al.* (2005), for example, mapped out the sills in the sedimentary basins of the distal Møre and Vøring margins offshore Norway and showed that the intruded region has a total areal extent

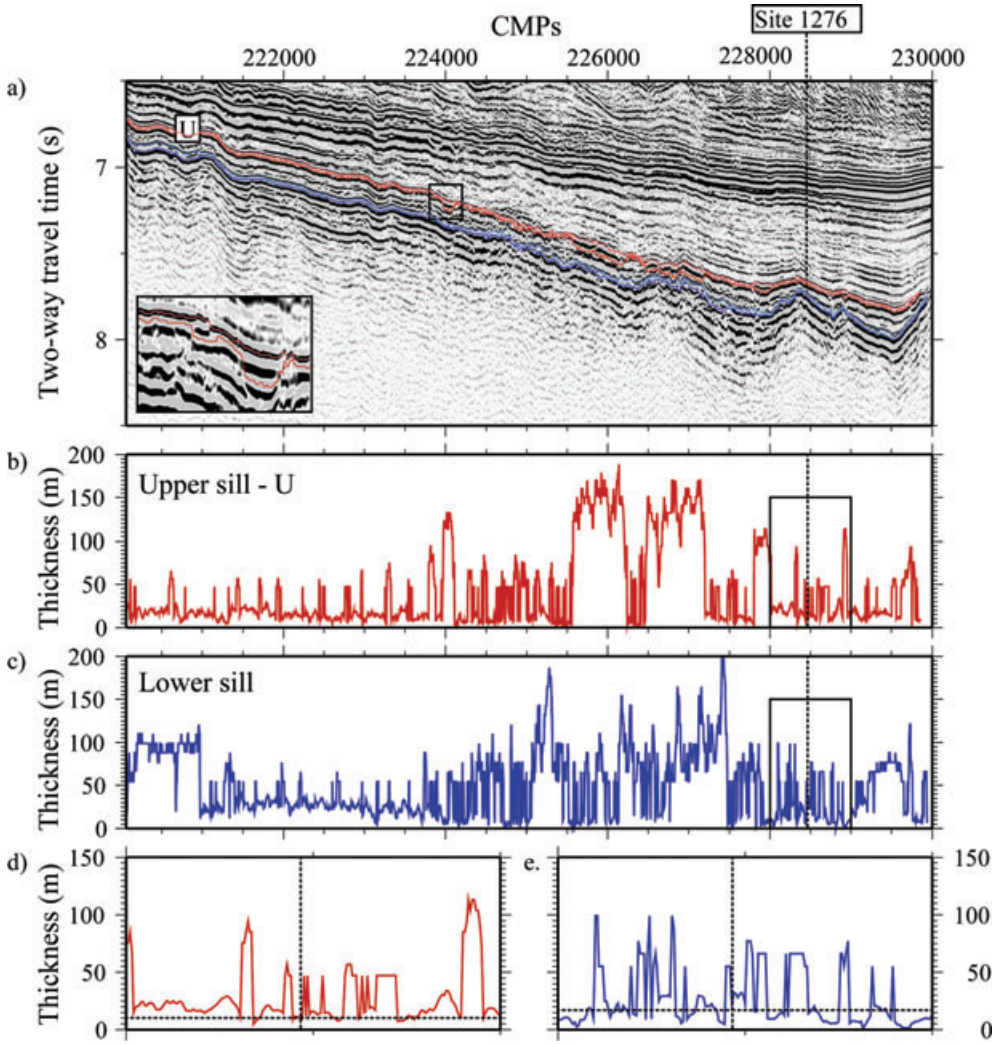

Figure 13. (a) Segment of the SCREECH 2 MCS reflection profile with interpretations of the top and base of the upper sill marked by red dotted and solid lines, respectively; the top of the sill is coincident with the U reflection. Similar interpretations are shown in blue for the lower sill. The inset shows an area of interpreted thickening of the upper sill indicated by changes in amplitude and polarity. This change in attributes could either reflect the thickening of a single sill or the presence of multiple sills at this level. Vertical exaggeration is ~10. (b) Thickness of upper sill (red) along SCREECH 2. (c) Thickness of the lower sill (blue) along SCREECH 2. Each sill appears to be 20–30 m thick along much of the line, with larger thicknesses up to ~150 m in a few places. (d) Expanded view of estimated thickness of the upper sill near Site 1276. Vertical dotted line shows location of the drill site, and horizontal dotted line shows thickness of upper sill (10 m) at the site. (e) Expanded view of estimated thickness of lower sill near Site 1276. Vertical dotted line shows location of the drill site, and horizontal dotted line shows recovered thickness of lower sill (17 m) at the site; drilling did not fully penetrate the sill, so its full thickness is not known.

of 82 000 km^2; the volume of the sill complex there is on the order of 9000 to 28 000 km^3.

Calculating a total volume of magmatic intrusions on the Newfoundland margin is subject to numerous uncertainties, but we can make some minimum and maximum estimates. A rough minimum value can be obtained if we assume that the area of interpreted sills contains only a single sill of 10 m thickness (i.e. equivalent to the upper sill drilled at Site 1276), in which case the volume would be ~800 km^3. Including a lower sill that is equivalent to the >17 m thick sill at Site 1276 would increase this minimum to ~2160 km^3.

A maximum value, admittedly unrealistic, can be derived if we assume that the entire high-amplitude reflection sequence is igneous rock. This sequence is defined to lie between sills at the U reflection and either the interpreted basement or the base of the high-amplitude reflections where underlying sediments are distinguishable above basement (Section 3.1). If we apply a mean velocity of 5.5 km s^{-1} (an average *P*-wave velocity for sill intrusions (Berndt *et al.* 2000) and for the lower sill at Site 1276 (Tucholke *et al.* 2004) to the observed traveltime thickness of this sequence along all the MCS lines studied, calculated actual thickness ranges from ~50 to ~1200 m, with a mean value of ~480 m. Combining this with the observed area of sills in the basin gives a total volume of ~38 400 km^3.

A more realistic approximation of actual volume can be obtained if we apply the estimate from the SCREECH 2 profile (Section 5.2.3) that about 26 per cent of the interval with high-amplitude reflections is igneous. Assuming a somewhat lower average sill velocity of 4.75 km s^{-1} (i.e. an average of the velocities of the upper and lower sills at Site 1276) and an average sediment velocity of 2.6 km s^{-1} as measured between the sills at the site (Tucholke *et al.* 2004), the average velocity of the interval is 3.16 km s^{-1}. Using this velocity, total sequence thickness is ~28 to ~700 m, with a mean value of ~280 m. Applying the 26 per cent factor, total igneous rock thickness ranges from ~7 to ~180 m, with a mean of ~73 m. Thus, the total volume of igneous rock would be ~5800 km^3. In Fig. 14,

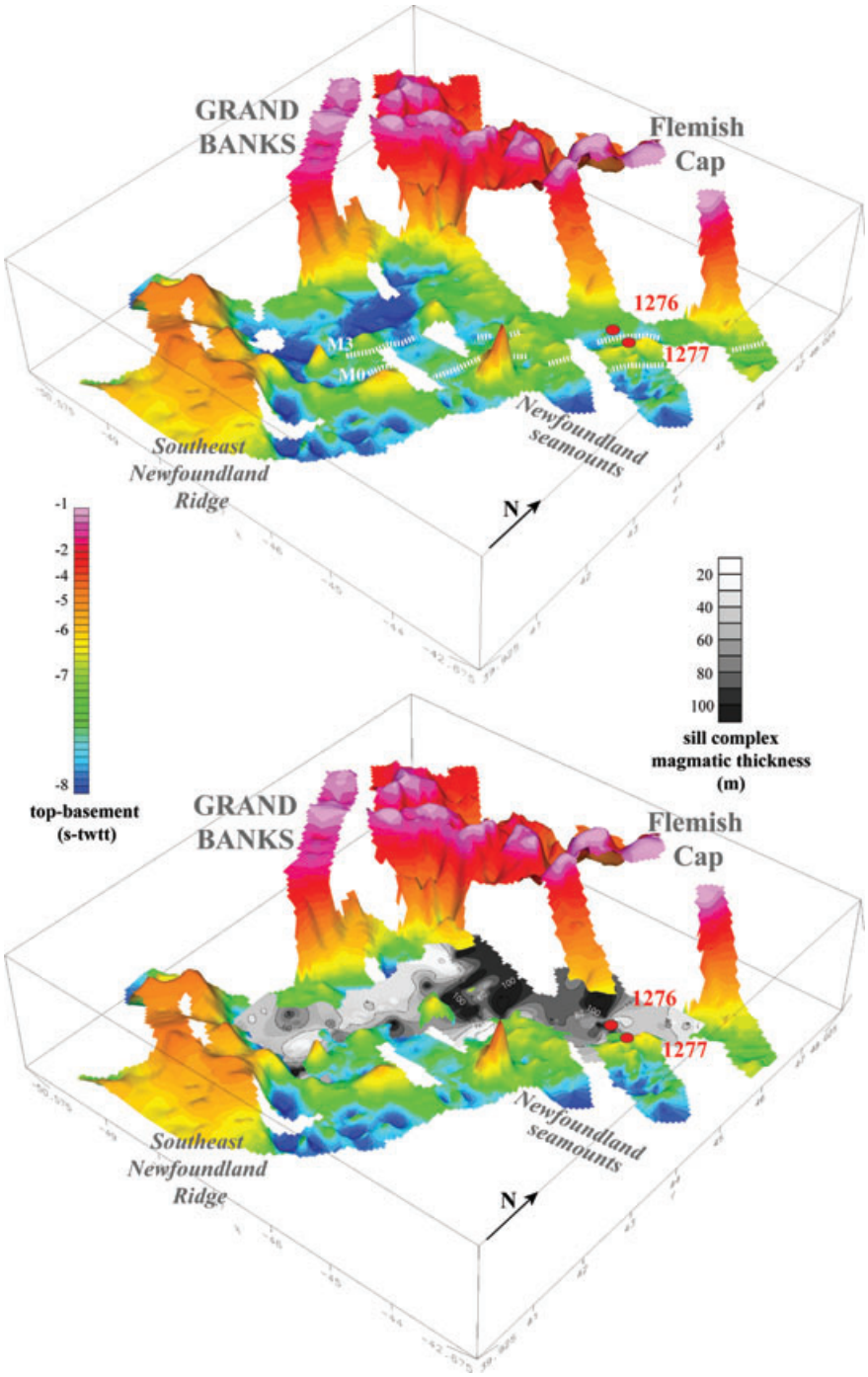

Figure 14. Top panel: 3-D view of top-basement (the plan-view map is in Fig. 3). Bottom panel: 3-D view of top-basement with estimated aggregate thickness of igneous rocks intruded as sills above basement, up to and including the U reflection (grey scale). The igneous thickness represents the 'most likely' hypothesis described in the text. Contour interval for igneous thickness is 20 m. Gridding and display are as noted for Fig. 3. Magnetic anomalies M3 and M0, and ODP Sites 1276 and 1277 are indicated.

we show a contour map of aggregate thickness of igneous sills in the Newfoundland Basin based on this last estimate.

Our minimum (~800 to 2160 km^3) and maximum (~38 400 km^3) estimates for the volume of the sill complez span a huge range, but they at least provide some limits on post-rift magmatism along the Newfoundland margin. The high-end value clearly is a gross overestimate, exceeding even the maximum volume that Planke *et al.* (2005) derived for the volcanic Møre-Vøring margins. Our 'most likely' estimate of ~5800 km^3 is a little more than half of the minimum estimated for Møre-Vøring. Even if the actual igneous volume in the Newfoundland Basin is closer to our estimated minimum, it represents a significant amount of post-rift magmatism along a margin that was essentially non-volcanic during its rifting phase.

6.2 Source of magma for the sill complex

There are several possible sources of magma for the post-rift sills drilled at Site 1276. Below we consider three hypotheses on the

potential sources of magmatism around the Newfoundland margin and compare them to our observations and other previously published data.

6.2.1 Tectonism along a fracture zone

Pe-Piper *et al.* (1994, 2007) suggested that Cretaceous magmatism documented in wells on the southern Grand Banks and Scotian shelf, and at the adjacent Fogo Seamounts along the southern transform margin of the Grand Banks, was related to tectonism along the Newfoundland Fracture Zone (FZ). They proposed that plate motion during opening of the Newfoundland–Iberia rift was not orthogonal to the Newfoundland FZ and that this created a leaky transform with magmatism driven by edge-controlled convection. Igneous rocks recovered in these locations have isotopic signatures of ocean island basalts with or without a continental component, and the compositions are distinct from those expected from plume sources.

There are several reasons why this scenario is unlikely to account for sill injection in the Newfoundland Basin. First, all the igneous rocks considered by Pe-Piper *et al.* (2007) have ages that are at least ∼10–20 Myr older than the sills (Fig. 2). Secondly, there are no known fracture zones with significant age offset in the Newfoundland Basin, so it would not be expected that plate-motion changes would stimulate magmatism in leaky transforms there. Even if the lithosphere was 'leaky' because plate-motion changes affected smaller-scale defects in the plate, it would be hard to explain why such magmatism occurred only in the Newfoundland Basin without also affecting the conjugate lithosphere of the Iberia margin where no comparable magmatism is observed. Thirdly, if the post-rift magmatism in the Newfoundland Basin originated only from a leaky Newfoundland FZ, a southward increase in the thickness of post-rift igneous rocks would be expected in the basin, whereas our results clearly demonstrate that magmatism was concentrated farther north in the area of the Newfoundland Seamounts. Finally, the diabases forming the Newfoundland sills are geochemically distinct from the igneous rocks reported by Pe-Piper *et al.* (2007); unlike those rocks, the Sr, Nd and Pb isotopes of the Site 1276 sills suggest an enriched hotspot/plume mantle source (Hart & Blusztajn 2006).

6.2.2 Mantle plume

Duncan (1984) proposed that the Newfoundland Seamounts and the Southeast Newfoundland Ridge were formed by magmatism associated with the migration of the Azores, Madeira and Canary plumes across the region between about 110 and 80 Ma (Fig. 9), and Karner & Shillington (2005) proposed that these plumes could be responsible for the post-rift sill intrusions in the Newfoundland Basin. Here we consider possible relationships between sill emplacement and passage of the Newfoundland Basin lithosphere over each of the plumes.

First we consider magmatism that formed the JAR–MTR, as described in Section 2. According to the reconstructions of Duncan (1984), the JAR–MTR conjugates (Fig. 1a) were formed along the Newfoundland–Iberia rift axis and southward along the Mid-Atlantic Ridge axis above the Canary plume between about 100 and 90 Ma. However, drilling on the JAR showed that basement there was emplaced by early Aptian time (ca. 125 Ma) (Shipboard Scientific Party 1979). Although there may have been some later magmatism at the JAR that was associated with passage of the Canary plume, it must have been minor in comparison to the initial ridge-building phase and it therefore would be an unlikely source for the voluminous sill magmatism in the Newfoundland Basin to the north. Furthermore, if the Canary plume were responsible for the sill intrusion, we would expect the strongest sill development to be near and above the plume track across the southern part of the rift (Fig. 9), not in the area of the Newfoundland Seamounts to the north.

A second possible source for the Newfoundland sills is the Azores plume. The reconstructions of Duncan (1984) indicate that the Azores plume passed beneath the Newfoundland Basin, but the projected time of plume passage is ∼70 Ma and younger. This was more than ∼25 Myr after the sills at Site 1276 were emplaced, which rules out the Azores plume as a viable source. It is noteworthy, however, that passage of this plume might help to explain young ages that Jagoutz *et al.* (2007) found for the plagioclases in the Newfoundland Basin (Fig. 2). Thermal effects of this plume could have reset the ages, and/or limited magmatism may have been associated with its passage.

Finally, the Newfoundland sill intrusions may have been related to magmatism associated with the Madeira plume. Duncan's (1984) projection is that transitional crust in the Newfoundland Basin passed over this plume at ∼90 Ma, which is slightly younger than the sill ages. The only radiometric date on lavas from the Newfoundland Seamounts (97.7 ± 1.5 Ma, Sullivan & Keen 1977; SMT in Fig. 2) is generally consistent with the proposed track of the Madeira plume and is the same as the age of the younger sill at Site 1276. In addition, sill magmatism in the Newfoundland Basin appears to have been centred at and north of the Newfoundland Seamounts (Figs 9 and 14), further suggesting a connection to the Madeira plume. Duncan (1984) proposed that the Newfoundland–Iberia rift axis did not pass over the Madeira plume until <80 Ma. If this was the case, the Madeira plume would not have affected Iberia transitional basement, which is older than ∼112 Ma. This is consistent with the lack of sills on the Iberia margin.

However, the primary difficulty with invoking the Madeira plume to account for the sill magmatism is that the older, 105 Ma sill was emplaced >10 Myr before (and >300 km ahead) of the calculated arrival of the plume at the western edge of the Newfoundland Basin. If the Madeira plume indeed was the magma source, the most likely explanations for this discrepancy are: (1) the calculated plume track is ca. 10 Myr in error, and/or (2) the plume was not a point source but instead consisted of two or more sources within a ∼150 km radius. Considering that plume 'tracks' may be hundreds of kilometres wide (Geldmacher *et al.* 2001) and that track ages calculated by different authors (e.g. Morgan 1983; Duncan 1984) can differ by 10 Myr or more, these explanations are reasonable. It should also be noted that wide-angle seismic data from the Newfoundland Basin (Funck *et al.* 2003; Lau *et al.* 2006b; Van Avendonk *et al.* 2006) show no evidence for significant mafic underplating, which might be expected to be associated with the passage of a mantle plume. However, it is possible that magma, rather than forming an underplate, was retained in the mantle as gabbroic intrusions, as is observed in slow-spreading oceanic crust (Lizarralde *et al.* 2004; Kelemen *et al.* 2006); incomplete melt extraction from the mantle also could have occurred, as described at the hotspot-influenced Reykjanes Ridge (Gaherty & Dunn 2007). Conventional interpretation of basement velocities in the Newfoundland basin is that the transition zone is highly thinned continental crust and exhumed serpentinized mantle, but either of the aforementioned processes could reduce mantle velocities to develop the observed velocity structure. Resolving this issue will require a combination of further geophysical studies and drilling.

6.2.3 Off-axis magmatism during early seafloor spreading

We also consider a third, new hypothesis in which off-axis magmatism was stimulated by thermal/compositional perturbations associated with the end of rifting and the gradual organization of magmatism at the new mid-ocean ridge axis.

Assuming a half spreading rate of 10–13 mm yr^{-1} (Sibuet *et al.* 2007), the spreading axis would have been 250–325 km seaward of the eastern edge of the transition zone (anomaly M3/4, 130 Ma) at the time the first sill was injected at ∼105 Ma, and it would have been ∼320–415 km seaward when the second sill was emplaced at ∼98 Ma. Although off-axis magmatism associated with mature mid-ocean ridges is usually restricted to within ∼10 km of the ridge axis (Dusunur *et al.* 2009), there are scenarios in which it might have been possible for magma either to be generated off-axis or to migrate and be expressed preferentially on the Newfoundland side of the basin because of long-distance channelling effects (e.g. Breivik *et al.* 2008). Moreover, at the Aden margin for instance, recent investigations (Lucazeau *et al.* 2009) demonstrate that the ocean–continent transition of the northern rifted margin contains an active centre of magmatism long after break-up (18 Myr) and at a significant distance from the ridge (220 km). Thus, complicated 3-D variations in lithospheric thickness, that are expected to arise from rifting, may influence and guide the migration of magmas from the mid-ocean ridge or other magmatic sources (Ebinger & Sleep 1999; Cannat *et al.* 2009; Shillington *et al.* 2009).

In addition, numerical models suggest that convection cells and thermal anomalies induced by rifting can persist for tens of millions of years after continental separation (Boutillier & Keen 1999). In fact, geochemistry and dating of rocks recovered at Site 1277 on the Newfoundland margin and at transition-zone drill-sites on the conjugate Iberia margin imply the continuation of a complicated off-axis magmatic/hydrothermal system long after the cessation of rifting (Jagoutz *et al.* 2007). If small-scale convection instabilities were present in the widening rift, low-degree decompression melting could have been associated with these cells at the lithosphere–asthenosphere boundary. Peron-Pinvidic and Manatschal (2009); Van Avendonk *et al.* (2009) hypothesized that mantle rocks on the outer parts of the Newfoundland and Iberia margins were exhumed from beneath Newfoundland, which could have favoured the genesis of such instabilities under that margin.

We expect that the total volume of magmatic material resulting from waning, rift-induced thermal anomalies, and/or off-axis MOR magmatism would be more modest than what would be expected from a plume, which would be consistent with the apparent lack of underplating noted in the previous section. According to this scenario, magmatism associated with the Madeira plume would have been restricted almost entirely to formation of the Newfoundland Seamounts.

6.3 Sill emplacement – constraints and effects

Based on the available seismic reflection data, seismically identifiable sills in the Newfoundland Basin are restricted entirely to the region of Barremian (anomaly M3) and older basement in the transitional domain. They appear not to have intruded sediments overlying continental crust except where such crust may be present in very thin allochthons at the western margin of transitional basement. As noted earlier, at the two times when sills at ODP Site 1276 were emplaced (∼105 and ∼98 Ma), the eastern boundary of the North American plate would have been some 250–415 km seaward of anomaly M3. Why are sills or other indications of magmatism not identified above this younger basement? There are several possible reasons. First, basement east of M3 is generally much rougher than the transitional basement; this makes it difficult to differentiate possible accumulations of late-stage magmatic products from pre-existing basement topography and mass-wasting deposits. Secondly, at the time of sill injection there was only thin sediment cover over the younger basement, in part because the rough, elevated topography blocked much of the downslope sediment transport from the Newfoundland margin. Intrusions or extrusives could have obliterated this thin sedimentary record, creating a seismic basement that is indistinguishable from true basement. Finally, magmatism may not have affected this basement simply because melt supply was waning and/or intermittent.

A remarkable aspect of the Newfoundland sills is that they almost all occur at or below the U reflection. Assuming that all the upper sills were injected at a level of hydrostatic equilibrium, their confinement to a common depth at the U reflection suggests that they were all emplaced at about the same time, that is ∼105 Ma as at Site 1276. In addition, the basin-wide distribution of sills at U indicates that this was a robust magmatic event. Confinement of younger sills (e.g. the ∼98 Ma sill at Site 1276) to deeper levels despite a thicker sediment overburden (and thus a shallower equilibrium level) might be an effect of the earlier sills 'capping' subsequent melt injection. Alternately, later magmatism may have been weaker and unable to force melts to shallow levels; this would be consistent with the idea that magmatism was waning over time and thus had little effect in areas of younger basement.

Drilling at Site 1276 showed that the sedimentary interval between the two sills was underconsolidated (most strongly in the lower 30 m of the section), but it was not overpressured (Tucholke *et al.* 2004). This suggests that the upper sill probably had considerable physical support provided by nearby dikes or pipes, as schematically illustrated in Fig. 15. As a consequence, sediments beneath the upper sill would not have been fully compacted by the load of later sedimentary overburden, and fluids would have been only partially vented upward through the sill. Other areas in the basin could be quite different. For example, if the upper sill had

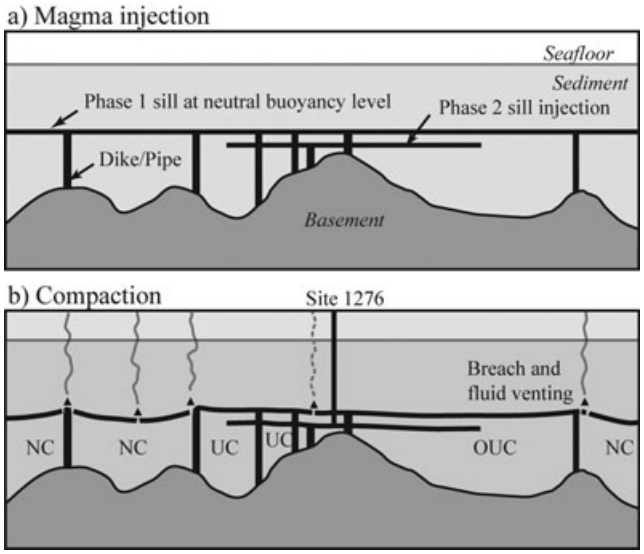

Figure 15. Schematic illustration of (a) sill injection and (b) subsequent venting of hydrothermal fluids and compaction of sediments below the upper sill. See text for discussion. NC, normally consolidated; UC. underconsolidated; OUC, overpressured and underconsolidated.

little support and significant breaches (Fig. 15, left side), the sill would have settled and underlying sediments would be normally consolidated; venting of fluids could be expressed by concentrated or diffuse disruption of the overlying sediments depending on whether there were a few large breaks or smaller, more dispersed breaches in the sill. We commonly observe convex-downward sills between local highs in the sills, together with indications of co-located venting in the overlying sediments, which may reflect this configuration (Figs 6c–d and 8). It is also possible that in some areas a 'cell' of sediments is effectively sealed beneath the sill (Fig. 15, right side). In this case, the sill should be nearly flat, there should be no indication of fluid venting, and sediments below the sill may be both underconsolidated and overpressured.

7 CONCLUSIONS

The Newfoundland and Iberia conjugate margins are considered to be an archetype of 'magma-poor' rifting, with wide zones of serpentinized mantle exhumed during a period of transitional extension before normal seafloor spreading began. However, the inner zone of transitional basement on the Newfoundland margin was affected by widespread post-rift magmatism, in strong contrast to the conjugate Iberia transitional basement where no significant post-rift magmatism is known. We used MCS reflection profiles and seismic signal analysis to study the nature, distribution, and origin of the magmatism on the Newfoundland margin. Our principal observations are summarized as follows.

1. Features interpreted as igneous sills are widely observed in the deepest part of the sedimentary column within the western part of the Newfoundland Basin. They occur over an area of ∼80 000 km^2 above Lower Cretaceous (older than anomaly M3, ∼130 Ma) transitional basement that consists of serpentinized mantle and possibly of very thin continental crust along the western basin margin.

2. The shallowest sills were almost all emplaced at the level of the U reflection which, together with the correlative 'orange reflection' on the Iberia margin, has been interpreted as a stratigraphic marker recording onset of relatively normal seafloor spreading near the Aptian–Albian boundary (∼112 Ma). The uniform level of the shallow sills suggests that they were all intruded at about the same time and at a common level of hydrostatic equilibrium. One of these sills was drilled at ODP Site 1276 and has been dated at ∼105 Ma (middle Albian; Hart & Blusztajn 2006). The widespread distribution of the shallow sills in the Newfoundland Basin suggests that this was a major magmatic event.

3. Strong reflections in the section below the shallowest sills indicate that numerous sills were also intruded there. One of these deeper sills was drilled at Site 1276 and dated at ∼98 Ma (Hart & Blusztajn 2006). It seems likely that many, if not most of the deeper sills in the basin were intruded following the ∼105 Ma event. They may have been restricted to the deeper levels because they were 'capped' by the shallow sills, because the later magmatism was weaker, or both.

4. Observed sill features include high-amplitude reflections with the following geometries: step-like forms, minor transgressive features, abrupt terminations, marked lateral disruptions in reflection amplitude, junctions between reflections, finger-like geometries, and local highs that may represent loci of magma injection in otherwise flat sills.

5. Disrupted reflections in sediments above the sills, interpreted as effects of hydrothermal venting, occur in numerous subvertical zones that are restricted to the Albian—lower Turonian section. This sedimentary section is capped by a condensed and eroded section representing a lacuna that has uncertain duration but is potentially up to ∼10 Myr. Depending on the duration of this lacuna and the time of last sill injection, the venting persisted for at least ∼6 Myr and possibly as much ∼23 Myr after sill emplacement.

6. Using synthetic seismograms, we estimated the total aggregate thickness of sills along one of the major seismic reflection dip lines crossing the basin (SCREECH 2). The results suggest that intrusions comprise ∼26 per cent of the section between basement and the top of the upper sills. Applying this result to profiles across the remainder of the basin where sills are observed, we obtain a very rough estimate of ∼5800 km^3 for the total volume of igneous rocks emplaced as sills in the sedimentary sequence by post-rift magmatism.

7. The source of the magma for the sills is still uncertain. Geospatial, geochemical and age data are consistent with a source from the Madeira plume. Alternately, or in addition, the magmatism may have been generated by asymmetric rift-drift related tectono-magmatic processes.

ACKNOWLEDGMENTS

Two anonymous reviewers provided pertinent and useful comments that helped us revised and improved our manuscript. G. Peron-Pinvidic's post-doctoral research at the University of Strasbourg and Woods Hole Oceanographic Institution was supported by TOTAL. D.J. Shillington thanks the University of Strasbourg for supporting her as a visiting scientist in May-June 2007, during which time she worked on this project. Part of the work presented here was also completed while Shillington was a post doc at the National Oceanography Center, Southampton. B. Tucholke's research was supported by NSF grant OCE0647035. Multichannel seismic field programs that provided much of the data used for this research were supported by NSF grants OCE839085, OCE830823 and OCE9819053.

REFERENCES

Abe, N., 2001. Petrochemistry of serpentinized peridotite from the Iberia Abyssal Plain (ODP Leg 173): its character intermediate between sub-oceanic and sub-continental upper mantle, in *Non-Volcanic Rifting of Continental Margins: A Comparison of Evidence from Land and Sea,* Vol. 187, pp. 143–159, eds Wilson, R.C.L., Whitmarsh, R.B., Taylor, B. & Froitzheim, N., Geological Society of London, London.

Afilhado, A., Matias, L., Shiobara, H., Hirn, A., Mendes-Victor., L. & Shimamura, H., 2008. From unthinned continent to ocean: the deep structure of the West Iberia passive continental margin at 38°N., *Tectonophysics,* **458,** 9–50; doi:10.1016/j.tecto.2008.03.002.

Berndt, C., Skogly, O.P., Planke, S., Eldholm, O. & Mjelde, R., 2000. High-velocity break-up related sills in the Vøring Basin off Norway, *J. geophys. Res.,* **105**(B12), 28 443–28 455.

Boillot, G. *et al*., 1987a. *Proceedings of the Ocean Drilling Program, Initial Reports,* Vol. 103, p. 663, Ocean Drilling Program, College Station, TX.

Boillot, G. *et al*., 1987b. Tectonic denudation of the upper mantle along passive margins: a model based on drilling results (ODP leg 103, western Galicia margin, Spain), *Tectonophysics,* **132,** 335–342.

Boutillier, R.R. & Keen, C.E., 1999. Small-scale convection and divergent plate boundaries, *J. geophys. Res.,* **104,** 7389–7403.

Bown, J.W. & White, R.S., 1995. Effect of finite extension rate on melt generation at rifted continental margins, *J. geophys. Res.,* **100,** 18 011–18 029.

Breivik, A.J., Faleide J.I. & Mjelde, R., 2008. Neogene magmatism northeast of the Aegir and Kolbeinsey ridges, NE Atlantic: spreading ridge–mantle plume interaction? *Geochem. Geophys. Geosyst.,* **9,** Q02004, doi:10.1029/2007GC001750.

Brown, A.R., Wright, R.M., Burkart, K.D., Abriel, W.L. & McBeath, R.G., 1986. Tuning effects, lithological effects and depositional effects in the seismic response of gas reservoirs, *Geophys. Prospect.,* **34,** 623–647.

Cannat, M., Manatschal, G., Sauter D. & Peron-Pinvidic, G., 2009. Assessing the conditions of continental breakup at magma-poor rifted margins: what can we learn from slow-spreading mid-ocean ridges?, *C. R. Geosci. Special Issue,* **341**(5), 406–427, doi:10.1016/j.crte.2009.01.005.

Chian, D., Louden, K.E., Minshull, T.A. & Whitmarsh, R.B., 1999. Deep structure of the ocean-continent transition in the southern Iberian Abyssal Plain from seismic refraction profiles: ocean drilling program (legs 149 and 173) transect, *J. geophys. Res.,* **104,** 7443–7462.

Cornen, G., Beslier, M.O. & Girardeau, J., 1996. Petrologic characteristics of the ultramafic rocks from the ocean/continent transition in the Iberia Abyssal Plain, in *Proceedings of the ODP, Scientific Results,* Vol. 149, eds Whitmarsh, R.B., Sawyer, D.S., Klaus, A. & Masson, D, Ocean Drilling Program, College Station, TX.

Dean, S.M., Minshull, T.A., Whitmarsh, R.B. & Louden, K.E., 2000. Deep structure of the ocean-continent transition in the southern Iberia Abyssal Plain from seismic refraction profiles: the IAM-9 transect at 40°20'N, *J. geophys. Res.,* **105,** 5859–5885.

Deemer, S., Hall, J., Solvason, K., Lau, K.W.H., Srivastava, S. & Sibuet, J.C., 2009. Structure and development of the southeast Newfoundland continental passive margin: derived from SCREECH Transect 3, *Geophys. J. Int.,* **178,** 1008–1020.

Driscoll, N.W., Hogg, J.R., Karner, G.D. & Christie-Blick, N., 1995. Extensional tectonics in the Jeanne d'Arc basin: implications for the timing of break-up between Grand Banks and Iberia, in *The Tectonics Sedimentation and Paleoceonography of the North Atlantic Region,* Geol. Soc., London, Special Publication, **90,** pp. 1–28, eds Scrutton, R.A., Stoker, M.S., Shimmield, G.B. & Tudhope, A.W., Geological Society, London.

Duncan, R.A., 1984. New England seamount age progression, *J. geophys. Res.,* **89,** 9980–9990.

Dusunur, D. *et al*., 2009. Seismological constraints on the thermal structure along the Lucky Strike segment (Mid-Atlantic Ridge) and interaction of tectonic and magmatic processes around the magma chamber, *Mar. geophys. Res,* **30**(2), 105–120, doi: 0.1007/s11001-009-9071-3.

Ebinger, C.J. & Sleep, N.H., 1998. Cenozoic magmatism throughout east Africa resulting from impact of a single plume, *Nature,* **395,** 788–791, doi: 10.1038/27417.

Enachescu, M.E., 1988. Extended basement beneath the intracratonic rifted basins of the Grand Banks of Newfoundland, *Can. J. Explor. Geophys.,* **24,** 48–55.

Francis, E.H., 1982. Magma and sediment emplacement mechanism of late carboniferous tholeiite sills in the northern Britain, *J. geol. Soc. Lond.,* **139,** 1–20.

Fuchs, K. & Müller, G., 1971. Computation of synthetic seismograms with the reflectivity method and comparison with observations, *Geophys. J. R. astr. Soc.,* **23,** 417–433.

Funck, T., Hopper, J.R., Larsen, H.C., Louden, K.E., Tucholke, B.E. & Holbrook, W.S., 2003. Crustal structure of the ocean-continent transition at Flemish Cap: seismic refraction results, *J. geophys. Res.,* **108,** doi:10.1029/2003JB002434.

Gaherty, J.B. & Dunn, R.A. 2007. Evaluating hotspot-ridge interaction in the Atlantic from regional-scale seismic observations, *Geochem. Geophys. Geosyst.,* **8,** Q05006, doi:05010.01029/GC001533.

Geldmacher, J., Hoernle, K., Van Den Bogaard, P., Zankl, G. & Garbe-Schönberg, D., 2001. Earlier history of the ≥70-Ma-old Canary hotspot based on the temporal and geochemical evolution of the Selvagen Archipelago and neighboring seamounts in the eastern North Atlantic, *J. Volc. Geotherm. Res.,* **111**(1–4), 55–87.

Geldmacher, J., Hoernle, K., Klugel, A., von der Bogaard, P., Wombacher, F. & Berning, B., 2006. Origin and geochemical evolution of the Madeira-Tore Rise (eastern North Atlantic), *J. geophys. Res.,* **111**(B9), doi:10.1029/2005JB003931.

Gradstein, F.M. *et al*., 2004. *A Geologic Time Scale 2004.* Cambridge University Press, Cambridge.

Grange, M., Schärer, U., Cornen, G. & Girardeau, J., 2008. First alkaline magmatism during Iberia–Newfoundland rifting, *Terra Nova,* **20,** 494–503.

Grant, A.C., 1977. Multichannel seismic reflection profiles of the continental crust beneath the Newfoundland Ridge, *Nature,* **270,** 22–25.

Greenberg, M.L. & Castagna, J.P., 1992. Shear-wave velocity estimation in porous rocks—theoretical formulation, preliminary verification and applications, *Geophys. Prospect.,* **40**(2), 195–209.

Groupe, G., 1979. The continental margin off Galicia and Portugal: acoustical stratigraphy, dredge stratigraphy, and structural evolution, in *Initial Reports of the Deep Sea Drilling Project,* pp. 633–662, **47**, Part II, eds Sibuet, J.C., *et al*., US Government Printing Office, Washington, DC.

Hansen, D.M. & Cartwright, J., 2006. Saucer-shaped sill with lobate morphology revealed by 3D seismic data: implications for resolving a shallow-level sill emplacement mechanism, *J. geol. Soc. Lond.,* **163,** 509–523.

Hart, S.R. & Blusztajn, J., 2006. Age and geochemistry of the Mafic Sills, ODP Site 1276, Newfoundland Margin, *Chem. Geol.,* **235,** 222–237.

Hébert, R., Gueddari, K., Lafleche, M.R., Beslier, M.-O. & Gardien, 2001. Petrology and geochemistry of exhumed peridotites and gabbros at non-volcanic margins: ODP Leg 173 West Iberia ocean-continent transition zone, in *Non-Volcanic Rifting of Continental Margins: A Comparison of Evidence from Land and Sea,* Geol. Soc., London, Special Publications, **187,** pp. 161–189, eds Wilson, R.C.L., Whitmarsh, R.B., Taylor, B. & Froitzheim, N, Geological Society, London.

Hopper, J.R., Funck, T., Tucholke, B.E., Larsen, H.C., Holbrook, W.S., Louden, K.E., Shillington, D. & Lau, H., 2004. Continental breakup and the onset of ultra-slow spreading off Flemish Cap on the Newfoundland rifted margin, *Geology,* **32,** 93–96.

Hopper, J.R., Funck, T., Tucholke, B.E., Louden, K., Holbrook, S. & Larsen, H.C., 2006. A deep seismic investigation of the Flemish Cap margin: implications for the origin of deep reflectivity and evidence for asymetric break-up between Newfoundland and Iberia. *Geophys. J. Int.,* **164,** 501–515.

Jagoutz, O., Müntener, O., Manatschal, G., Rubatto, D., Peron-Pinvidic, G., Turrin, B.D. & Villa, I.M., 2007. The rift-to-drift transition in the North Atlantic: a stuttering start of the MORB machine?, *Geology,* **35,** 1087–1090.

Journel, A.G. & Huijbregts, C.J., 1978. *Mining Geostatistics,* Academic Press, London.

Kallweit, R.S. & Wood, L.C., 1982. The limits of resolution of zero-phase wavelets, *Geophysics,* **47,** 1035–1046.

Karner, G.D. & Shillington, D.J., 2005. Basalt Sills of the 'U Reflector': a serendipitous dating technique, *Geology,* **33,** 985–988.

Kelemen, P.B., Kikawa, E., Miller, D.J. & Shipboard Scientific party., 2006. Leg 209 Summary: processes in a 20-km-thick conductive boundary layer beneath the Mid-Atlantic Ridge, 14°-16°N, in *Proceedings of the ODP Science Research, Vol. 209: College Station,* eds Kelemen, P.B., Kikawa, E. & Miller, D.J., Ocean Drilling Program, TX.

Kennett, B.L.N., 1983. *Seismic Wave Propagation in a Stratified Media,* p. 342 Cambridge University Press, Cambridge.

Lau, K.W.H., Louden, K.E., Deemer, S., Hall, J., Hopper, J.R., Tucholke, B.E., Holbrook, W.S. & Larsen, H.C., 2006a. Crustal structure across the Grand Banks – Newfoundland Basin continental margin (Part II) – Results from a seismic reflection profile, *Geophys. J. Int.,* **167,** 157–170.

Lau, K.W.H., Louden, K.E., Funck, T., Tucholke, B.E., Holbrook, W.S., Hopper, J.R. & Larsen, H.C., 2006b. Crustal structure across the Grand Banks – Newfoundland Basin continental margin (Part I) – results from a seismic refraction profile, *Geophys. J. Int.,* **167,** 127–156.

Lavier, L.L. & Manatschal, G., 2006. A mechanism to thin the continental lithosphere at magma-poor margins, *Nature,* **440,** 324–328.

Lizarralde, D., Gaherty, J.B., Collins, J.A., Hirth, G. & Kim, S.D., 2004. Spreading-rate dependence of melt extraction at mid-ocean ridges from mantle seismic refraction data, *Nature,* **432,** 744–747.

Lucazeau, F. *et al*., 2009. Post-rift volcanism and high heat-flow at the ocean-continent transition of the eastern Gulf of Aden, Terra Nova, **21,** 285–292, doi: 10.1111/j.1365-3121.2009.00883.x.

Marfut, K.J. & Kirlin, R.L., 2001. Narrow-band spectral analysis and thin-bed tuning, *Geophysics,* **66,** 1274–1283.

Merle, R., Scharer, U., Girardeau, J., Cornen, G., 2006. Cretaceous seamounts along the continent-ocean transition of the Iberian margin: U-Pb ages and Pb-Sr-Hf isotopes, *Geochim. Cosmochim. Acta,* **70,** 4950–4976.

Minshull, T.A. & Singh, S.C., 1993. Shallow structure of oceanic crust in the Western North Atlantic from seismic waveform inversion and modeling, *J. geophys. Res.,* **98,** 1777–1792.

Morgan, W.J., 1983. Hotspot tracks and the early rifting of the Atlantic, *Tectonophysics,* **94,** 123–139.

Müntener, O. & Manatschal, G., 2006. High degrees of melt extraction recorded by spinel harzburgites of the Newfoundland margin: the role of inheritance and consequences for the evolution of the North Atlantic, *Earth planet. Sci. Lett.,* **252,** 437–452.

Pe-Piper, G., Jansa, L.F. & Palacz, Z., 1994. Geochemistry and regional significance of the Early Cretaceous bimodal basalt-felsic associations on Grand Banks, eastern Canada, *Bull. geol. Soc. Am.,* **106,** 1319–1331.

Pe-Piper, G., Piper, D.J.W., Jansa, L.F. & de Jonge, A., 2007. Early Cretaceous opening of the North Atlantic Ocean: implications of the petrology and tectonic setting of the Fogo Seamounts off the SW Grand Banks, Newfoundland, *Bull. geol. Soc. Am.,* **119,** 712–724.

Peron-Pinvidic, G. & Manatschal, G., 2009. The final rifting evolution at deep magma-poor passive margins: a new point of view based on observations from Iberia-Newfoundland, *Int. J. Earth Sci.,* 98-7, 2009, doi: 10.1007/s00531-008-0337-9.

Peron-Pinvidic, G., Manatschal, G., Minshull, T. & Sawyer, D., 2007. The tectono-sedimentary and morpho-tectonic evolution recorded in the deep Iberia-Newfoundland margins: evidence for a complex break-up history, *Tectonics,* **26,** TC2011, doi:10.1029/2006TC001970.

Planke, S., Rasmussen, T., Rey, S.S. & Myklebust, R., 2005. Seismic characteristics and distribution of volcanic intrusions and hydrothermal vent complexes in the Vøring and Møre basins, in *Petroleum Geology: North-West Europe and Global Perspectives – Proceedings of the 6th Petroleum Geology Conference,* pp. 833–844, eds Doré, A.G. & Vining, B., Geological Society, London.

Pross, J., Pletsch, T., Shillington, D.J., Ligouis, B., Schellenberg, F. & Kus, J., 2007. Thermal alteration of terrestrial palynomorphs in mid-Cretaceous organic-rich mudstones intruded by an igneous sill (Newfoundland Margin, ODP Hole 1276A), *Int. J. Coal Geol.,* **70,** 277–291.

Puryear, C.I. & Castanga, J.P., 2008. Layer-thickness determination and stratigraphic interpretation using spectral inversion: theory and application, *Geophysics,* **73,** R37–R48.

Rabinowitz, P.D., Cande, S.C. & Hayes, D.E., 1978. Grand Banks and J-Anomaly Ridge, *Science,* **202,** 71–73.

Réhault, J.P. & Mauffret, A., 1979. Relationships between tectonics and sedimentation around the northwestern Iberian margin, Initial Reports of the Deep Sea Drilling Project, 47 (Pt.2), pp. 663–681, U.S. Government Printing Office, Washington, DC.

Russell, S.M. & Whitmarsh, R.B., 2003. Magmatism at the West Iberia non-volcanic rifted continental margin; evidence from analyses of magnetic anomalies, *Geophys. J. Int.,* **154,** 706–730.

Sawyer, D.S. *et al*., 1994. In *Proceedings of the ODP,* Initial Reports, Ocean Drilling Program, College Station, TX.

Shillington, D.J., Holbrook, W.S., Van Avendonk, H.J.A., Tucholke, B.E., Hopper, J.R., Louden, K.E., Larsen, H.C. & Nunes, G.T., 2006. Evidence for asymmetric nonvolcanic rifting and slow incipient oceanic accretion from seismic reflection data on the Newfoundland margin, *J. geophys. Res.,* **111,** doi:10.1029/2005JB003981.

Shillington, D.J., Tucholke, B.E., Karner, G.D., Sawyer, D.S., Holbrook, W.S. & Delius, H., 2007. Linking core and seismic data without logs: core-seismic correlation at site 1276, in *Proceedings of the ODP Science Results,* Vol. 210, eds Tucholke, B.E., Sibuet, J.-C. & Klaus, A., Ocean Drilling Program, College Station, TX.

Shillington, D.J., Hopper, J.R. & Holbrook, W.S., 2008. Seismic signal penetration beneath post-rift sills on the Newfoundland rifted margin, *Geophysics,* **73,** B99–B107, doi:10.1190/1.2972131.

Shillington, D.J., Scott, C.L., Minshull, T.A., Edwards, R.A., Brown, P.J. & White, N., 2009. Abrupt transition from magma-starved to magma-rich rifting in the eastern Black Sea, *Geology,* **37,** 7–10.

Shipboard Scientific Party, 1979. Site 384: the Cretaceous-Tertiary boundary, Aptian reefs, and the J-Anomaly ridge, Initial Reports of the Deep Sea Drilling Project, pp. 107–154, eds Tucholke, B.E. & Vogt, P.R., Government Printing Office, U.S. Washington, DC.

Sibuet, J. C., Srivastava, S. & Manatschal, G., 2007. Exhumed mantle-forming transitional crust in the Newfoundland-Iberia rift and associated magnetic anomalies, *J. geophys. Res.,* **112**(B6), doi:10.1029/2005JB003856.

Srivastava, S.P., Sibuet, J.C., Cande, S., Roest, W.R. & Reid, I.D., 2000. Magnetic evidence for slow seafloor spreading during the formation of the Newfoundland and Iberian margins, *Earth planet. Sci. Lett.,* **182,** 61–76.

Sullivan, K.D. & Keen, C.E., 1977. Newfoundland Seamounts: petrology and geochemistry, in *Volcanic Regimes in Canada,* pp. 461–476, eds Baragar, W.R.A., Coleman, L.C. & Hall, J.M., Geological Association of Canada Special Paper 16.

Tankard, A.J., Welsink, H.J., and Jenkins, W.A.M., 1989. Structural Styles and Stratigraphy of the Jeanne d'Arc Basin, Grand Banks of Newfoundland, in *Extensional Tectonics and Stratigraphy of the North Atlantic Margins,* pp. 265–282, eds Tankard, A.J. & Balkwill, H.R., American Association of Petroleum Geologists, AAPG Memoir 46: Tulsa, OK.

Thomson, K. & Hutton, D., 2004. Geometry and growth of sill complexes: insights using 3D seismic from the North Rockall Trough, *Bull. Volc.*, **66,** 364–375.

Tucholke, B.E. & Ludwig, W.J., 1982. Structure and origin of the J Anomaly Ridge, western North Atlantic Ocean, *J. geophys. Res.,* **87,** 9389–9407.

Tucholke, B.E. & Sibuet, J.C., 2007. Leg 210 synthesis: tectonic, magmatic, and sedimentary evolution of the Newfoundland-Iberia rift, in *Proceedings of the Ocean Drilling Program, Scientific Results,* Vol. 210, pp. 1–56, eds Tucholke, B.E. J.-C. Sibuet & Klaus, A., doi:10.2973/odp.proc.sr.210.101.2007, Ocean Drilling Program, College Station, TX.

Tucholke, B.E., Austin, J.A. & Uchupi, E., 1989. Crustal structure and rift-drift evolution of the Newfoundland Basin, in *Extensional Tectonics and Stratigraphy of the North Atlantic Margins,* AAPG Memoir 46, pp. 247–263, eds Tankard, A.J. & Balkwill, H.R., American Association of Petroleum Geologists, Tulsa, OK.

Tucholke, B.E. *et al*., 2004. In *Proceedings of the ODP,* Initial Reports, Vol. 210. Ocean Drilling Program, College Station, TX, doi:10.2973/odp.proc.ir.210.2004.

Tucholke, B.E., Sawyer, D.S. & Sibuet, J.C., 2007. Breakup of the Newfoundland-Iberia rift, in *Imaging, Mapping and Modelling Continental Lithosphere Extension and Breakup,* Geol. Soc., London, Special Publication, **282,** pp 9–46 eds Karner, G. Manatschal, G. & Pinheiro, L., Geological Society, London, doi: 10.1144/SP282.2.

Urquhart, E., Gardin, S., Leckie, R.M., Wood, S.A., Pross, J., Georgescu, M.D., Ladner, B. & Takata, H., 2007. A paleontological synthesis of ODP Leg 210, Newfoundland Basin, in *Proceedings of the ODP, Scientific Results,* Vol. 210, pp. 1–53, eds Tucholke, B. E., Sibuet, J.-C. & Klaus, A. Ocean Drilling Program, College Station, TX, doi:10.2973/odp.proc.sr.210.115.2007.

Van Avendonk, H.J.A., Holbrook, W.S., Nunes, G.T., Shillington, D.J., Tucholke, B.E., Louden, K.E., Larsen, H.C. & Hopper, J.R., 2006. Seismic velocity variations across the rifted margin of the eastern Grand Banks, Canada, *J. geophys. Res.,* **111,** B11404, doi:10.1029/2005JB004156.

Van Avendonk, H.J.A., Lavier, L., Shillington, D.J. & Manatschal, G., 2009. Extension of continental crust at the margin of the eastern Grand Banks, Newfoundland, *Tectonophysics,* **468**(1–4), 131–148, doi:10.1016/j.tecto.2008.05.030.

Whitmarsh, R.B. & Miles, P.R, 1995. Models of the development of the West Iberia rifted continental-margin at 40-degrees-30n deduced from surface and deep-tow magnetic-anomalies, *J. geophys. Res.,* **100**(B3), 3789–3806.

Whitmarsh, R.B., White, R.S., Horsefield, S.J., Sibuet, J.C., Recq, M. & Louvel, V., 1996. The ocean-continent boundary off the western continental margin of Iberia: crustal structure west of Galicia Bank, *J. geophys. Res.,* **1001(**B12), 28291–28314.

Whitmarsh, R.B. *et al*., 1998. In *Proceedings of the ODP,* Initial Report, Ocean Drilling Program, College Station, TX.

Whitmarsh, R.B., Manatschal, G. & Minshull, T.A., 2001. Evolution of magma-poor continental margins from rifting to seafloor spreading, *Nature,* **413,** 150–153.

Widess, M.B., 1973. How thin is a thin bed?, *Geophysics,* **38,** 1176–1180.

Wilson, R.C.L., Manatschal, G. & Wise, S., 2001. Rifting along nonvolcanic passive margins: stratigraphic and seismic evidence from the Mesozoic successions of the Alps and Western Iberia, in *Non-Volcanic Rifting of Continental Margins: A Comparison of Evidence from Land and Sea,* Geol. Soc., London, Special Publications, **187,** pp. 429–452, eds Wilson, R.C.L., Whitmarsh, R.B., Taylor, B. & Froitzheim, N., Geological Society, London.